Supporting Information for: Probing the Secrets of Hydrogen Bonding in the Crystal Structures of Organic Salt Phase Change Materials: the Origins of a High Enthalpy of Fusion

Samantha L. Piper,[a] Craig M. Forsyth,[a] Mega Kar,[b] Douglas R. MacFarlane,[a] Karolina Matuszek*[a] and Jennifer M. Pringle*[b]

[a]*School of Chemistry, Monash University, Clayton, Victoria 3800, Australia*
[b]*Institute for Frontier Materials, Deakin University, Burwood Campus, Burwood, Victoria 3125, Australia*

Emails: jenny.pringle@deakin.edu.au, karolina.matuszek@monash.edu

Table of contents

Supplemental figures

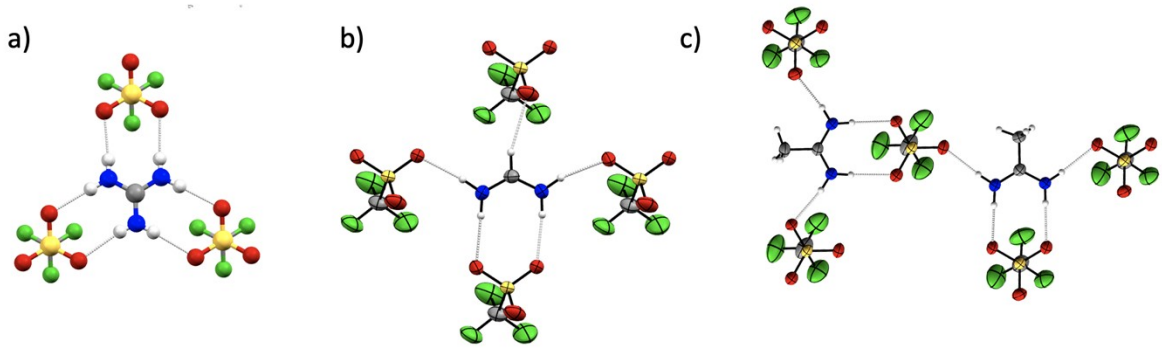

Figure S1. Crystallographically determined structures of [gdm][CF_3SO_3] **(a)**, [fa][CF_3SO_3] **(b)** and [aca][CF_3SO_3] **(c)**. Oxygen atoms are shown in red, sulfur atoms in yellow, carbon atoms

in grey, fluorine atoms in green, and nitrogen atoms in blue. Hydrogen atoms are shown as white spheres and hydrogen bonds are represented by broken grey lines.

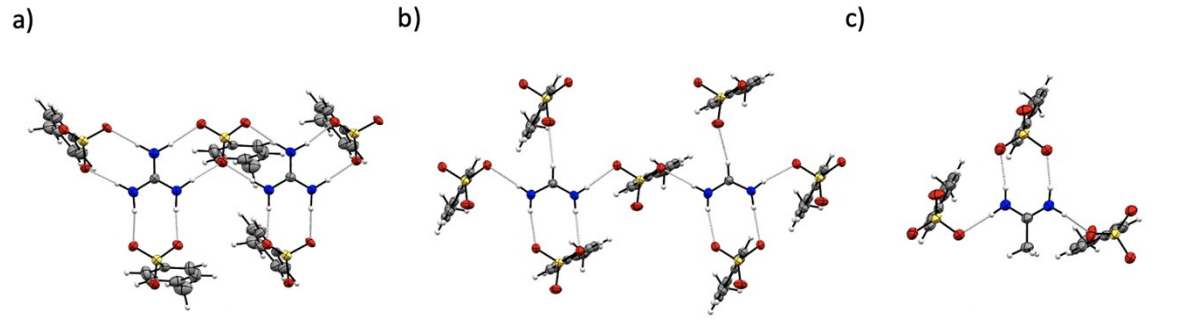

Figure S2. Crystallographically determined structures of [gdm][*p*-Tos] **(a)**, [fa][*p*-Tos] **(b)** and [aca][*p*-Tos] **(c)**. Oxygen atoms are shown in red, sulfur atoms in yellow, carbon atoms in grey, and nitrogen atoms in blue. Hydrogen atoms are shown as white spheres and hydrogen bonds are represented by broken grey lines.

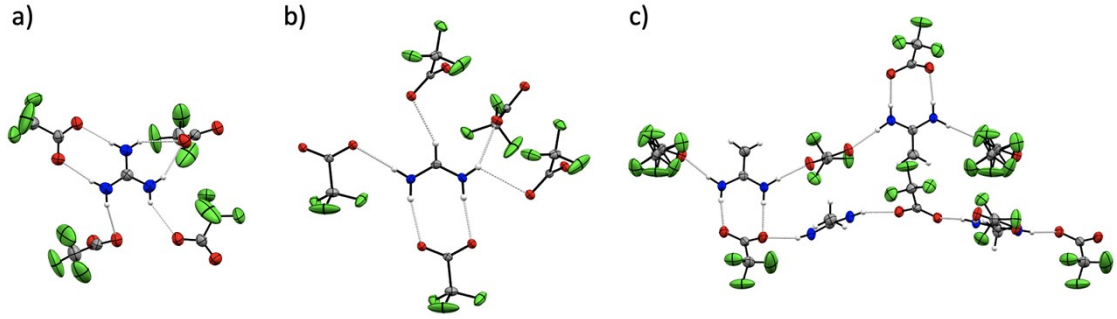

Figure S3. Crystallographically determined structures of [gdm][CF_3COO] **(a)**, [fa][CF_3COO] **(b)** and [aca][CF_3COO] **(c)**. Oxygen atoms are shown in red, carbon atoms in grey, fluorine atoms in green, and nitrogen atoms in blue. Hydrogen atoms are shown as white spheres and hydrogen bonds are represented by broken grey lines.

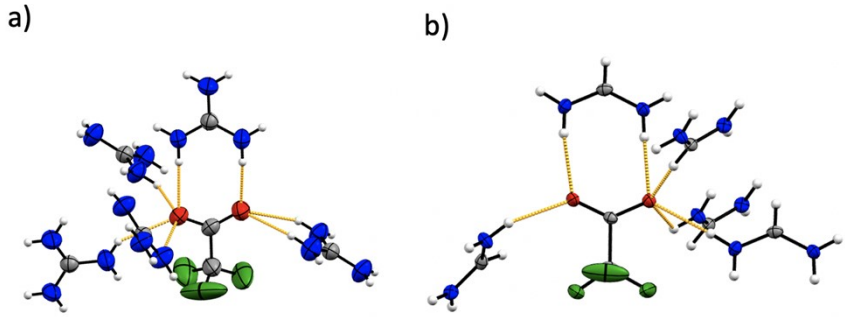

Figure S4. Trifluoroacetate anions in the structure of [gdm][CF_3COO] (a) and [fa][CF_3COO] (b), showing the bifurcated acceptor interactions, with one oxygen atom accepting four H-bonds

and one accepting three in [gdm][CF_3COO], and one oxygen atom accepting three H-bonds and the other two in [fa][CF_3COO]. Oxygen atoms are shown in red, carbon atoms in grey, fluorine atoms in green, and nitrogen atoms in blue. Hydrogen atoms are shown as white spheres and hydrogen bonds are represented by broken orange lines.

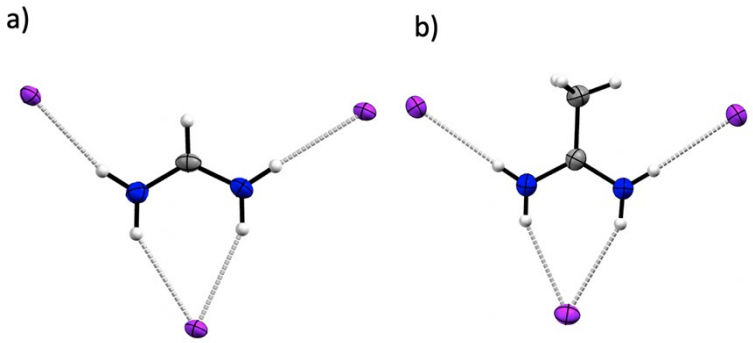

Figure S5. Crystallographically determined structures of [fa]Cl **(a)**, [aca]Cl **(b)**. Carbon atoms are shown in grey, nitrogen atoms in blue, chlorine atoms in purple, and hydrogen atoms in white. Hydrogen bonds are represented by broken grey lines.

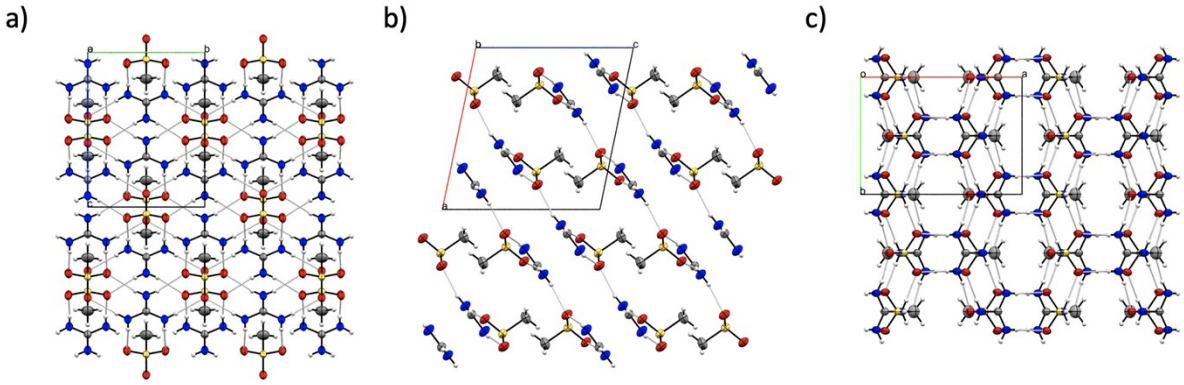

Figure S6. Extended crystal packing of [gdm][CH_3SO_3] down the a **(a)**, b **(b)**, and c **(c)** axis. Three unit cells are packed along each axis. Hydrogen bonds are represented by broken grey lines.

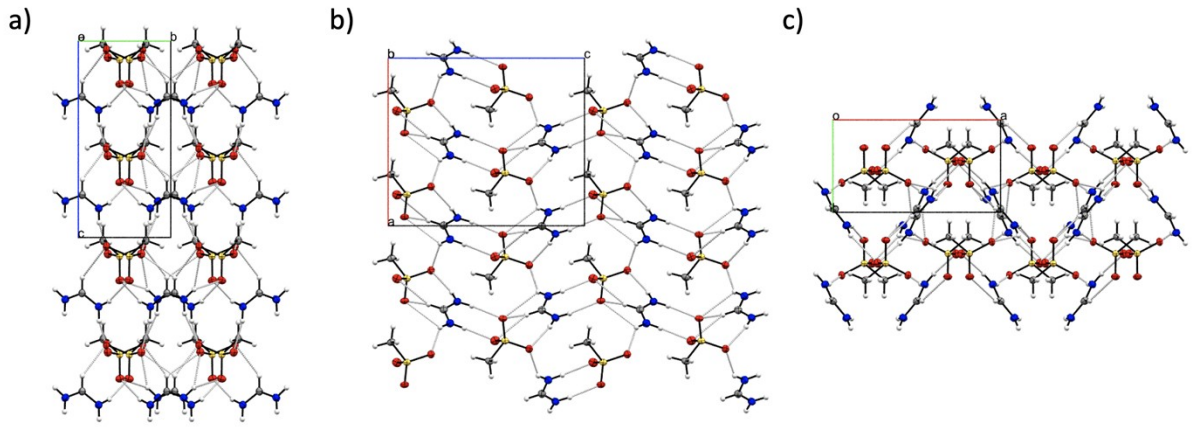

Figure S7. Extended crystal packing of [fa][CH_3SO_3] down the a **(a)**, b **(b)**, and c **(c)** axis. Three unit cells are packed along each axis. Hydrogen bonds are represented by broken grey lines.

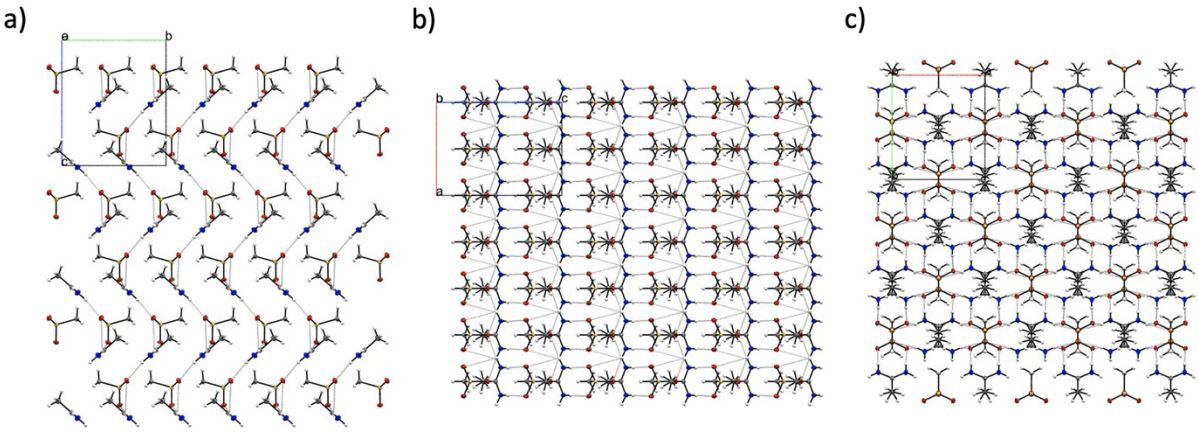

Figure S8. Extended crystal packing of [aca][CH_3SO_3] down the a **(a)**, b **(b)**, and c **(c)** axis. Three unit cells are packed along each axis. Hydrogen bonds are represented by broken grey lines.

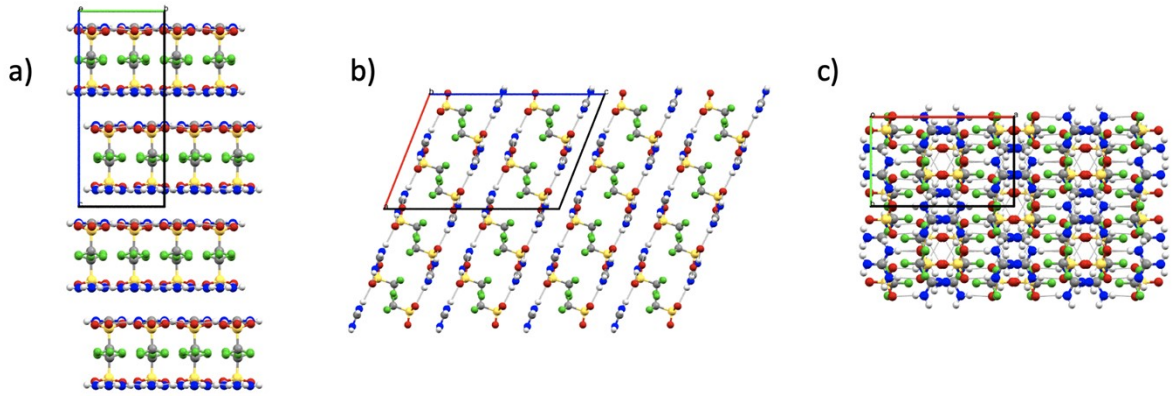

Figure S9. Extended crystal packing of [gdm][CF_3SO_3] down the a **(a)**, b **(b)**, and c **(c)** axis. Two unit cells are packed along each axis. Hydrogen bonds are represented by broken grey lines.

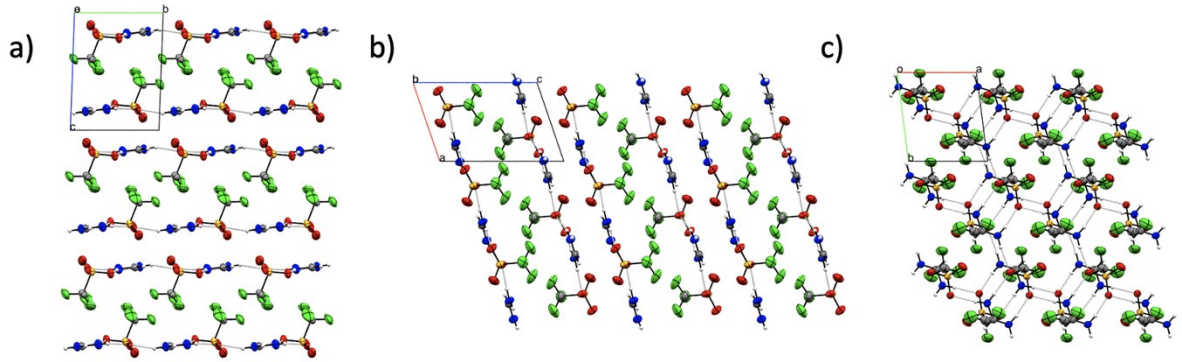

Figure S10. Extended crystal packing of [fa][CF_3SO_3] down the a **(a)**, b **(b)**, and c **(c)** axis. Three unit cells are packed along each axis. Hydrogen bonds are represented by broken grey lines.

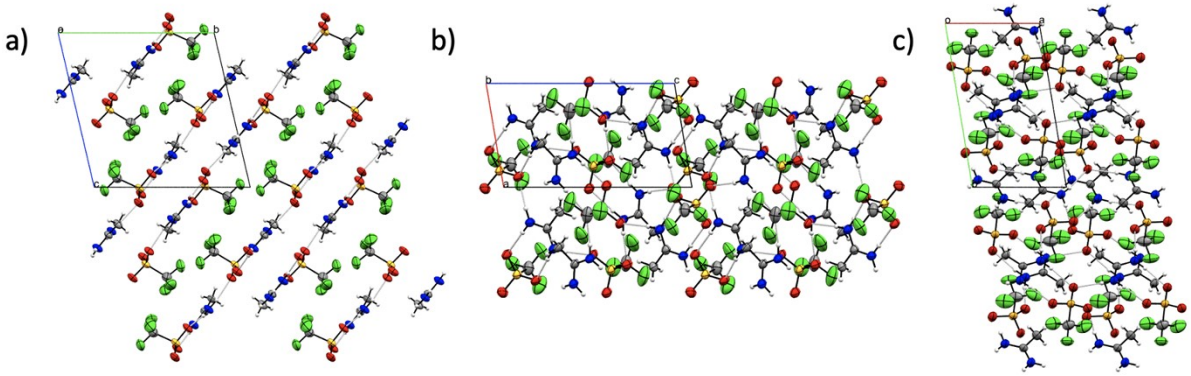

Figure S11. Extended crystal packing of [aca][CF_3SO_3] down the a **(a)**, b **(b)**, and c **(c)** axis. Two unit cells are packed along each axis. Hydrogen bonds are represented by broken grey lines.

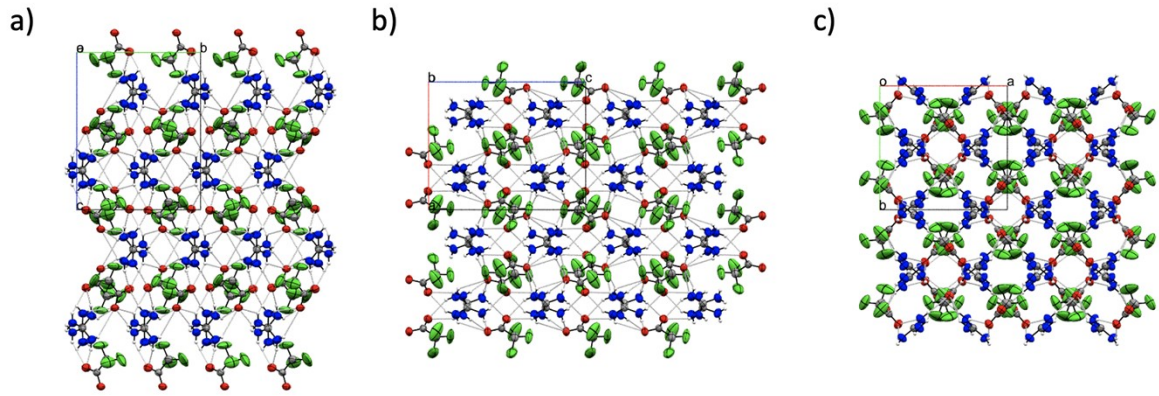

Figure S12. Extended crystal packing of [gdm][CF_3COO] down the a **(a)**, b **(b)**, and c **(c)** axis. Three unit cells are packed along each axis. Hydrogen bonds are represented by broken grey lines.

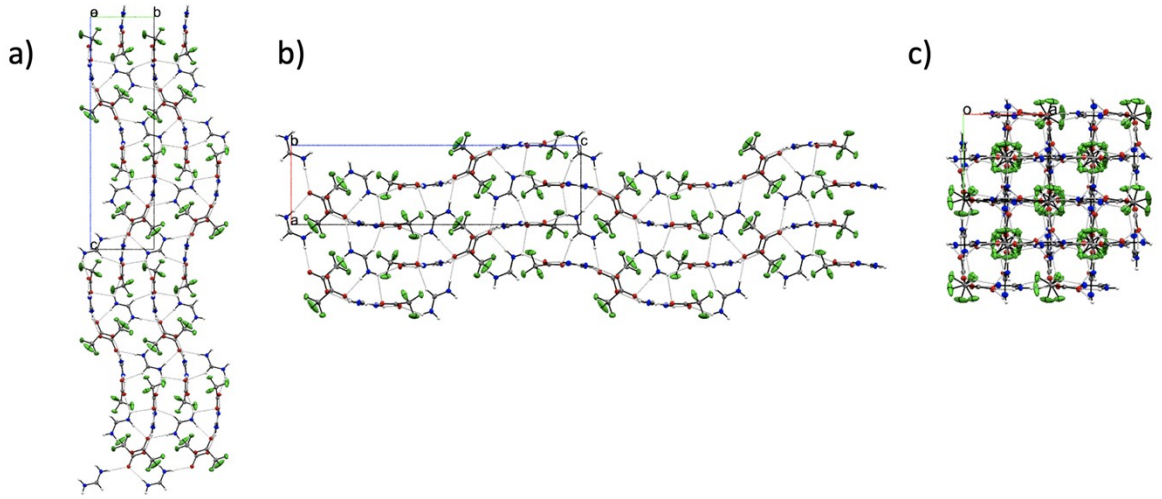

Figure S13. Extended crystal packing of [fa][CF_3COO] down the a **(a)**, b **(b)**, and c **(c)** axis. Two unit cells are packed along each axis. Hydrogen bonds are represented by broken grey lines.

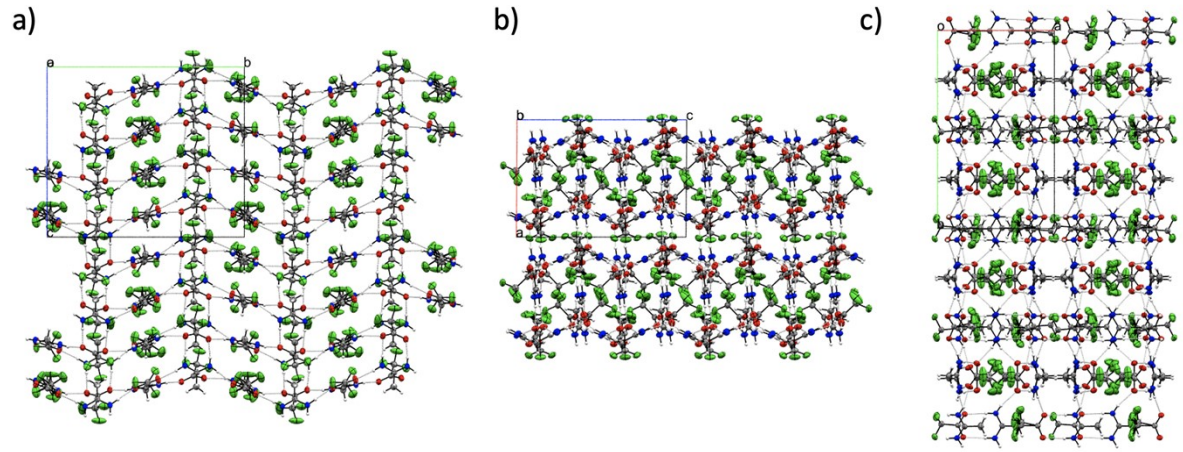

Figure S14. Extended crystal packing of [aca][CF_3COO] down the a **(a)**, b **(b)**, and c **(c)** axis. Two unit cells are packed along each axis. Hydrogen bonds are represented by broken grey lines.

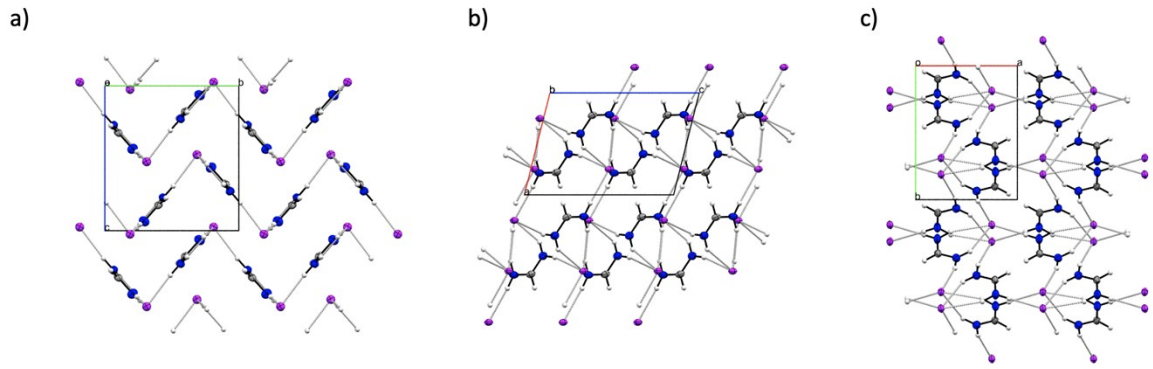

Figure S15. Extended crystal packing of [fa]Cl down the a **(a)**, b **(b)**, and c **(c)** axis. Two unit cells are packed along each axis. Hydrogen bonds are represented by broken grey lines.

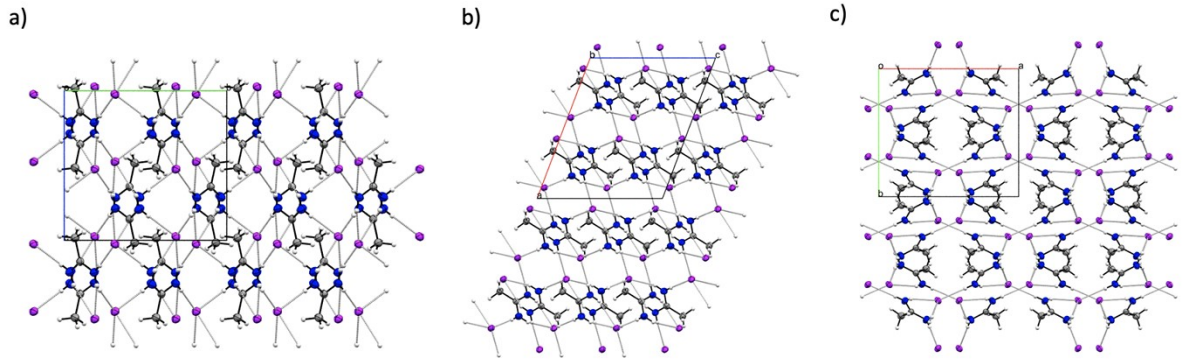

Figure S16. Extended crystal packing of [aca]Cl down the a **(a)**, b **(b)**, and c **(c)** axis. Two unit cells are packed along each axis. Hydrogen bonds are represented by broken grey lines.

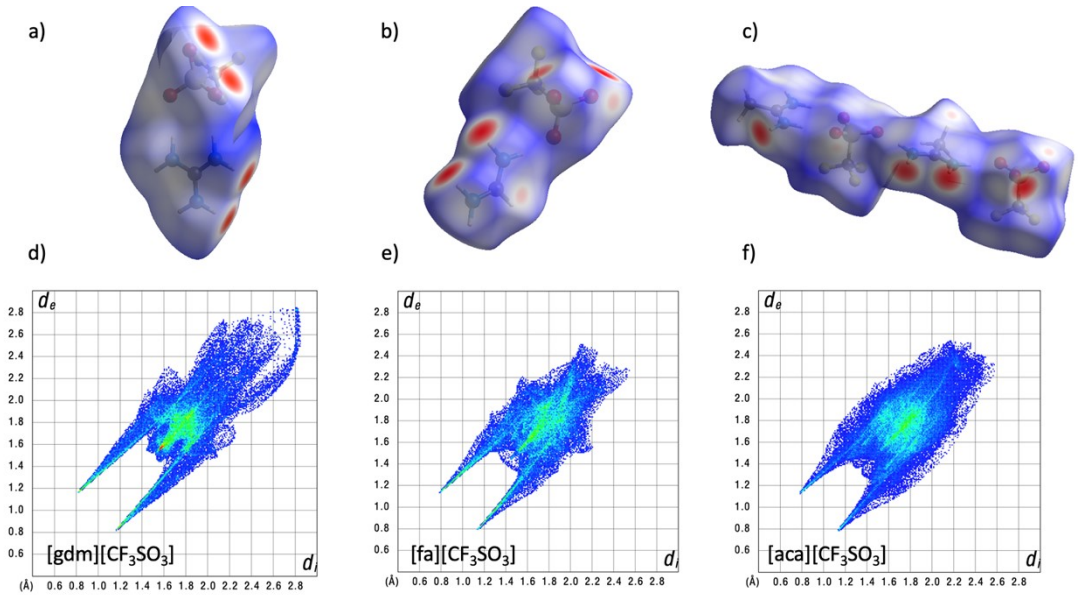

Figure S17. Hirshfeld surfaces and corresponding fingerprint plots of [gdm][CF_3SO_3] (a, d), [fa][CF_3SO_3] (b, e) and [aca][CF_3SO_3] (c, f).

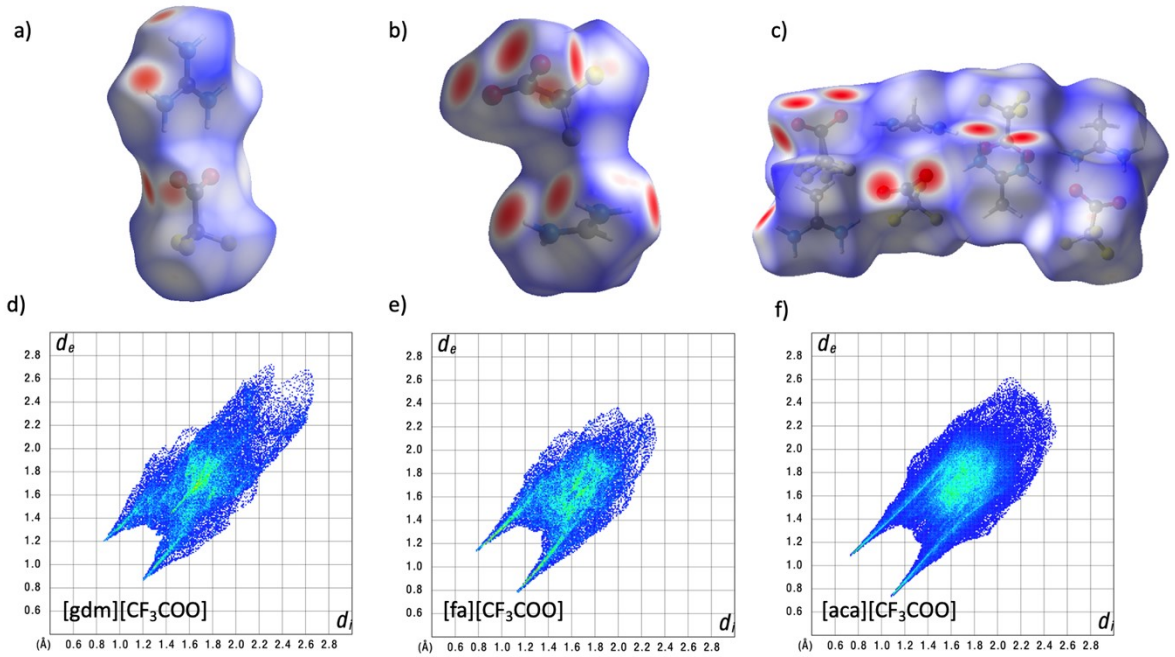

Figure S18. Hirshfeld surfaces and corresponding fingerprint plots of [gdm][CF_3COO] (a, d), [fa][CF_3COO] (b, e) and [aca][CF_3SCOO] (c, f).

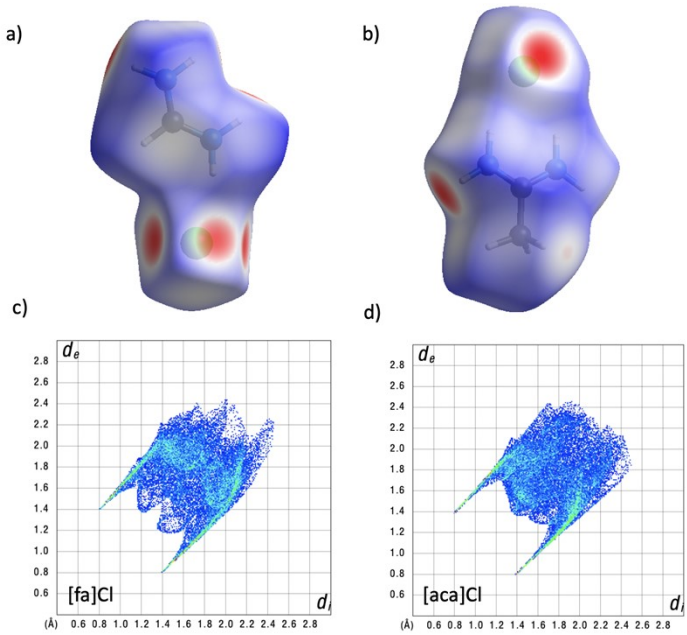

Figure S19. Hirshfeld surfaces **(a)** and **(b)** and corresponding fingerprint plots **(c)** and **(d)** of [fa]Cl, and [aca]Cl.

Literature data summary

Table S1. Thermal properties of [gdm][CH_3SO_3], [gdm][CF_3SO_3] and [gdm][*p*-Tos], as reported in the literature

Material	T_m **(°C)**	ΔH_m **(kJ/mol)**	T_{s-s} **(°C)**	ΔH_{s-s} **(kJ/mol)**
[gdm][CH_3SO_3][1]	208	29	-	-
[gdm][CF_3SO_3][1]	160	27	115	1
[gdm][*p*-Tos][1]	227	21	175	1

Table S2. Crystal system data and associated database identifiers and deposition numbers for crystal structures obtained through the Cambridge Crystallographic Data Centre (CCDC)

Material	**[aca]Cl**[2]	**[gdm][CF_3SO_3]**[3]	**[gdm][CF3COO]**[4]	**[gdm][*p*-Tos]**[5]
CCDC database identifier	ACIMDC01	WETNIS	IZIJEH01	HIBCAW01
CCDC deposition number	244747	1292511	2050456	883629
Space group	*C2/c*	*C2/c*	*Pbcn*	$P2_1/c$
a (Å)	11.5266(12)	12.988(7)	10.5705(13)	12.437(3)
b (Å)	9.8127(10)	7.512(2)	10.2525(13)	7.418(4)
c (Å)	9.6404(8)	18.45(1)	13.0173(15)	25.72(3)
α (°)	90	90	90	90
β (°)	110.732(5)	111.69(4)	90	95.56(6)
γ (°)	90	90	90	90

Materials and Methods

Synthesis

Formamidinium salts were synthesised by a salt metathesis reaction between formamidine hydrochloride (sourced from Sigma-Aldrich) and the silver salt of the respective anion. Formamidine hydrochloride was handled under a nitrogen atmosphere due to hygroscopicity. The two salts were combined in their stoichiometric ratios in an ethanolic solution and left to stir for 30 mins before the silver chloride by-product was removed by gravimetric filtration. The remaining ethanolic solution was concentrated by rotary evaporation and dried under high vacuum for > 4 hours. Synthesis of the product was confirmed by Nuclear Magnetic Resonance Spectroscopy (NMR):

[fa][CH_3SO_3]

^{1}H NMR (400 MHz, *d_6-DMSO*) δ 8.95 (s, 4 H), 7.87 (s, 1H), 2.42 (3H). **^{13}C NMR** (100.1 MHz, *d_6-DMSO*) δ 157.94.

[fa][CF_3SO_3]

^{1}H NMR (400 MHz, *d_6-DMSO*) δ 8.81 (s, 4 H), 7.84 (s, 1H). **^{13}C NMR** (100.1 MHz, *d_6-DMSO*) δ 157.7, 122.73, 119.53. **^{19}F NMR** (376.5 MHz, *d_6-DMSO*) δ -77.79.

[fa][*p*-Tos]

^{1}H NMR (400 MHz, *d_6-DMSO*) δ 8.87 (s, 5H), 7.86 (s, 1H), 7.50-7.48 (d, 2H), 7.14-7.12 (d, 2H), 2.30 (s, 3H). **^{13}C NMR** (100.1 MHz, *d_6-DMSO*) δ 157.76, 145.95, 138.24, 128.58, 125.94, 21.25.

[fa][CF_3COO]

^{1}H NMR (400 MHz, *d_6-DMSO*) δ 9.03 (s, 4 H,), 7.87 (s, 1H). **^{13}C NMR** (100.1 MHz, *d_6-DMSO*) δ 157.88, 119.14, 116.16. **^{19}F NMR** (376.5 MHz, *d_6-DMSO*) δ -73.68.

Acetamidinium salts were synthesised by a salt metathesis reaction between acetamidine hydrochloride (sourced from Sigma-Aldrich) and the silver salt of the respective anion. The two salts were combined in their stoichiometric ratios in an ethanolic solution and left to stir for 30 mins before the silver chloride by-product was removed by gravimetric filtration. The remaining ethanolic solution was concentrated by rotary evaporation and dried under high vacuum for > 4 hours. Synthesis of the product was confirmed by Nuclear Magnetic Resonance Spectroscopy (NMR):

[aca][CH_3SO_3]

^{1}H NMR (400 MHz, *d_6-DMSO*) δ 8.86-8.49 (d, 4H), 2.37 (s, 3H), 2.12 (s, 3H). **^{13}C NMR** (100.1 MHz, *d_6-DMSO*) δ 168.22, 18.73.

[aca][CF_3SO_3]

^{1}H NMR (400 MHz, *d_6-DMSO*) δ 8.85-8.31 (d, 4H), 2.11 (s, 3H). **^{13}C NMR** (100.1 MHz, *d_6-DMSO*) δ 168.10, 18.72. **^{19}F NMR** (376.5 MHz, *d_6-DMSO*) δ -77.76.

[aca][*p*-Tos]

^{1}H NMR (400 MHz, *d_6-DMSO*) δ 8.89-8.44 (d, 4H), 7.50-7.48 (d, 2H), 7.14-7.12 (d, 2H), 2.30 (s, 3H), 2.11 (s, 3H). **^{13}C NMR** (100.1 MHz, *d_6-DMSO*) δ 168.20, 145.96, 138.24, 128.58, 125.94, 21.25, 18.71.

[aca][CF_3COO]

^{1}H NMR (400 MHz, *d_6-DMSO*) δ 8.78 (s, 4H,), 2.11 (s, 3H). **^{13}C NMR** (100.1 MHz, *d_6-DMSO*) δ 168.33, 118.64, 115.66, 18.72. **^{19}F NMR** (376.5 MHz, *d_6-DMSO*) δ -73.71.

Guanidinium trifluoroacetate is a known material and was synthesised according to a known procedure.[6] **^{1}H NMR** (400 MHz, *d_6-DMSO*) δ 7.13 (s, 4H). **^{13}C NMR** (100.1 MHz, *d_6-DMSO*) δ 158.61, 119.03, 116.06. **^{19}F NMR** (376.5 MHz, *d_6-DMSO*) δ -73.80.

Crystallisations

Single crystals of [fa][Cl] were formed by heating a vial containing ~ 0.5 g [fa][Cl] and ~ 6 mL acetonitrile at 85 °C for 10 minutes in a Monowave 50. Upon cooling, needle crystals of [fa][Cl] formed on the walls of the vial. Single crystals of [fa][CF_3SO_3] were formed by dissolving a sample of the salt in ethanol and hexane (~10:1) and allowing the solution to sit at room temperature for ~ 4 weeks. All other crystals were obtained by dissolving the respective salts in ethanol, adding five drops of hexane, and refrigerating the samples. Crystals typically formed after > 3 days of refrigeration.

Characterisation

Differential Scanning Calorimetry details

Transition temperatures (melting, T_m and solid-solid, $T_{s\text{-}s}$) and thermal data (enthalpies of fusion, ΔH_f) were determined using a DSC 8000 Perkin-Elmer differential scanning calorimeter with a heating and cooling rate of 10 °C/min, with 1 minute isothermal at both temperature ends. 4 – 10 mg of sample was sealed in an aluminium pan for measurements. The equipment was calibrated using an indium (T_m = 156.6 °C, ΔH_f = 28.45 J/g) and cyclohexane (T_m = 8 °C) standards. Measurements were performed under a nitrogen atmosphere, with an N_2 flow rate of 50 mL/min, and performed in triplicate. Thermal properties were taken from the second heating/cooling cycle. T_m was determined by the peak maxima and ΔH_f was calculated by integrating the area under the endothermic transition curve, with Pyris software.

Nuclear Magnetic Resonance Spectroscopy (NMR)

^{1}H, ^{13}C{^{1}H} and ^{19}F{^{1}H} NMR spectra were recorded at 298 K on a Bruker Avance III NMR spectrometer equipped with a 9.4 T magnet and 5 mm TBO probe, operating at 400.13 MHz (^{1}H), 100.62 MHz (^{13}C), 376.48 MHz (^{19}F). Chemical shifts (δ) are reported in parts per million (ppm) and were referenced to the residual solvent signals (^{1}H, ^{13}C) or from the solvent block (^{2}H) signal according to IUPAC recommended secondary referencing method and the manufacturer's protocols (^{19}F).[7]

X-ray Crystallography

Crystal data and refinement details

Data for the [gdm] salts and [aca]Cl was obtained from the Cambridge Crystallographic Data Centre. Data for all other salts was collected on a Rigaku Xtalab Synergy Dualflex using a monochromator equipped with Cu–Kα (λ = 1.5418 Å) radiation, at 123 K. Data were processed using proprietary software CrysAlisPro.[8] All structures were solved any refined by the SHELX software suite[9,10] and refined against F^2 using Olex2[11] as a graphical interface. Non-hydrogen atoms were refined with anisotropic displacement parameters. Alkyl hydrogen atoms were included in calculated positions (riding model) and the amine protons were modelled on electron density with restrained N – H bond lengths of 0.91(2) Å using the DFIX restraint.

For [fa][CF_3SO_3], the unit cell parameters were determined at variable temperatures above and below the temperature of the solid-solid transition (123 K, 213 K, 253 K, 283 K). The unit cell parameters at each temperature are detailed in Table S5. The data modelled for analysis was collected at 123 K, after the sample was quench cooled to this temperature. When a crystal was slow cooled to 123 K, the quality of the data of too poor quality for refinement. For the data collected at 213 K, 253 K and 283 K, the crystal was cooled to the target temperature at a cooling rate of 10 °C/min.

The structure was of [aca][CF_3COO] was modelled as a 2-component morohedral twin using the twin law (1.0, 0.0, 0.0, 0.0, -1.0, 0.0, -0.015, 0.0, -1.0), with a batch scale factor (BASF) 0.074(1). Disorder of one of the CF_3 groups was modelled over 2 positions. The two disorder components had refined occupancies of 0.67 and 0.23. The bond distances were refined to be of equal distance using the SADI command.

The structure of [fa][CH_3SO_3] was refined as a racemic twin using the twin law (-1.0, 0.0, 0.0, 0.0, -1.0, 0.0, 0.0, 0.0, -1.0), with a batch scale factor (BASF) of 0.458. The CH_3 group of the anion was refined as a rotating group.

For the structure of [aca][CH_3SO_3], disorder of the CH_3 group of the acetamidinium cation was refined with riding coordinates over two positions corresponding to rotation of the CH_3 group, with occupancies of 0.5 for each hydrogen atom.

For the structure of [fa][*p*-Tos], the CH_3 groups of the toluene moieties of the two *p*-toluene sulfonate anions were refined as rotating groups.

Table S3. Crystal data and structure refinement details for [fa] salts

Identification code	**[fa][CH_3SO_3]**	**[fa][CF_3SO_3]**	**[fa][*p*-Tos]**	**[fa][CF_3COO]**	**[fa]Cl**
CCDC identifier	2090744	2090745	2090746	2090747	2090748
Empirical formula	$C_2H_8N_2O_3S$	$C_2H_5F_3N_2O_3S$	$C_{16}H_{24}N_4O_6S_2$	$C_3H_5F_3N_2O_2$	CH_5ClN_2
Formula weight/g.mol^{-1}	140.16	194.14	432.51	158.09	80.52

Temperature/K	122.99(10)	123.00(12)	123.00(10)	123.00(10)	123.01(10)
Crystal system	orthorhombic	triclinic	triclinic	tetragonal	monoclinic
Space group	Pca21	P-1	P-1	P41212	P21/c
a/Å	9.6440(3)	6.2803(3)	6.1440(2)	6.83933(6)	6.0881(3)
b/Å	5.3173(2)	6.7118(4)	12.8644(6)	6.83933(6)	7.7636(4)
c/Å	11.2997(3)	9.3224(6)	13.3576(3)	25.0216(4)	8.6548(4)
α/°	90	89.693(5)	89.604(3)	90	90
β/°	90	71.243(5)	85.602(3)	90	104.121(4)
γ/°	90	83.098(4)	82.341(3)	90	90
Volume/Å^3	579.45(3)	369.16(4)	1043.26(6)	1170.42(3)	396.71(3)
Z	4	2	2	8	4
***p* calc/g/cm^3**	1.607	1.747	1.377	1.794	1.348
μ/mm^{-1}	4.427	4.283	2.667	1.86	6.735
F(000)	296	196	456	640	168
Crystal size/mm^3	0.112 × 0.094 × 0.041	0.128 × 0.084 × 0.054	0.433 × 0.133 × 0.1	0.352 × 0.278 × 0.201	0.551 × 0.031 × 0.013
Radiation	Cu Kα (λ = 1.54184)	Cu Kα (λ = 1.54184)	Cu Kα (λ = 1.54184)	Cu Kα (λ = 1.54184)	Cu Kα (λ = 1.54184)
2Θ range for data collection/°	15.684 to 154.12	10.026 to 154.45	6.934 to 154.7	13.422 to 154.118	15.006 to 154.842
Index ranges	-10 ≤ h ≤ 12, -6 ≤ k ≤ 6, -10 ≤ l ≤ 14	-6 ≤ h ≤ 7, -8 ≤ k ≤ 8, -11 ≤ l ≤ 11	-7 ≤ h ≤ 7, -16 ≤ k ≤ 15, -16 ≤ l ≤ 15	-8 ≤ h ≤ 8, -8 ≤ k ≤ 8, -31 ≤ l ≤ 30	-7 ≤ h ≤ 3, -9 ≤ k ≤ 9, -10 ≤ l ≤ 10
Reflections collected	5410	7664	20728	12176	2554
Independent reflections	1023 [R_{int} = 0.0658, R_{sigma} = 0.0330]	1536 [R_{int} = 0.0602, R_{sigma} = 0.0344]	4317 [R_{int} = 0.0721, R_{sigma} = 0.0501]	1234 [R_{int} = 0.0309, R_{sigma} = 0.0126]	818 [R_{int} = 0.0567, R_{sigma} = 0.0554]
Data/restraints/parameters	1023/5/92	1536/4/116	4317/0/287	1234/4/108	818/4/57
Goodness-of-fit on F2	1.117	1.113	1.073	1.094	1.071
Final R indexes [I>=2σ (I)]	R1 = 0.0356, wR2 = 0.1002	R1 = 0.0693, wR2 = 0.1909	R1 = 0.0503, wR2 = 0.1406	R1 = 0.0384, wR2 = 0.1029	R1 = 0.0474, wR2 = 0.1301
Final R indexes [all data]	R1 = 0.0357, wR2 = 0.1003	R1 = 0.0735, wR2 = 0.1941	R1 = 0.0571, wR2 = 0.1466	R1 = 0.0389, wR2 = 0.1036	R1 = 0.0511, wR2 = 0.1344
Largest diff. peak/hole / e Å^{-3}	0.47/-0.50	0.91/-0.55	0.61/-0.62	0.38/-0.40	0.52/-0.60
Flack parameter	0.46(4)	-	-	0.04(6)	-

Table S4. Crystal data and structure refinement details for [aca] salts

Identification code	[aca][CH_3SO_3]	[aca][CF_3SO_3]	[aca][*p*-Tos]	[aca][CF_3COO]
CCDC identifier	2090749	2090750	2090751	2090752
Empirical formula	$C_6H_{20}N_4O_6S_2$	$C_3H_7F_3N_2O_3S$	$C_9H_{14}N_2O_3S$	$C_{16}H_{28}F_{12}N_8O_8$
Formula weight/g.mol^{-1}	308.38	208.17	230.28	688.46
Temperature/K	123.00(10)	122.99(10)	122.99(10)	123.00(10)
Crystal system	orthorhombic	triclinic	monoclinic	monoclinic
Space group	Cmc21	P-1	P21/c	P21/c
a/Å	7.69460(10)	6.5871(5)	14.4723(8)	10.7077(2)
b/Å	8.62580(10)	11.7652(7)	6.2210(3)	18.0846(3)
c/Å	10.37460(10)	11.9506(5)	14.2758(7)	15.5398(3)
α/°	90	74.772(5)	90	90
β/°	90	77.729(6)	115.747(7)	90.304(2)
γ/°	90	77.878(6)	90	90
Volume/Å^3	688.584(14)	861.47(10)	1157.68(12)	3009.15(10)
Z	2	4	4	4
p calc/g/cm^3	1.487	1.605	1.321	1.52
μ/mm^{-1}	3.778	3.713	2.435	1.495
F(000)	328.0	424.0	488.0	1408.0
Crystal size/mm^3	0.532 × 0.258 × 0.183	0.549 × 0.276 × 0.065	0.292 × 0.150 × 0.058	0.07 × 0.08 × 0.16
Radiation	Cu Kα (λ = 1.54184)	Cu Kα (λ = 1.54184)	Cu Kα (λ = 1.54184)	Cu Kα (λ = 1.54184)
2Θ range for data collection/°	15.432 to 154.476	7.776 to 159.03	12.428 to 153.864	7.5 to 155.014
Index ranges	-9 ≤ h ≤ 9, -10 ≤ k ≤ 10, -12 ≤ l ≤ 13	-7 ≤ h ≤ 8, -15 ≤ k ≤ 14, -11 ≤ l ≤ 15	-18 ≤ h ≤ 17, -7 ≤ k ≤ 4, -17 ≤ l ≤ 18	-13 ≤ h ≤ 13, -22 ≤ k ≤ 22, -19 ≤ l ≤ 12
Reflections collected	6711	17073	12134	29003
Independent reflections	767 [R_{int} = 0.0290, R_{sigma} = 0.0120]	3582 [R_{int} = 0.1136, R_{sigma} = 0.0648]	2398 [R_{int} = 0.0592, R_{sigma} = 0.0450]	6276 [R_{int} = 0.0527, R_{sigma} = 0.0429]
Data/restraints/parameters	767/3/57	3582/8/251	2398/4/192	6276/31/503
Goodness-of-fit on F2	1.094	1.113	1.064	1.079
Final R indexes [I>=2σ (I)]	R1 = 0.0232, wR2 = 0.0584	R1 = 0.0712, wR2 = 0.2062	R1 = 0.0599 wR2 = 0.1628	R1 = 0.0649, wR2 = 0.1855
Final R indexes [all data]	R1 = 0.0232, wR2 = 0.0584	R1 = 0.0801, wR2 = 0.2211	R1 = 0.0694, wR2 = 0.1744	R1 = 0.0751, wR2 = 0.2007
Largest diff. peak/hole / e Å^{-3}	0.19/-0.38	0.55/-0.86	0.86/-0.63	0.76/-0.52
Flack parameter	0.023(15)	-	-	-

Variable temperature unit cell data for [fa][CF_3SO_3]

Table S5. Unit cell data of [fa][CF_3SO_3] collected at 123 K, 213 K, 253 K, and 283 K

Unit cell parameters	**123 K**	**213 K**	**253 K**	**283 K**
a (Å)	6.2803(3)	6.2985(10)	6.3127(10)	6.185(2)
b (Å)	6.7118(4)	6.7176(9)	6.7116(10)	6.8170(13)
c (Å)	9.3224(6)	9.449(3)	9.523(3)	9.628(3)
α (°)	89.693(5)	89.445(17)	89.218(16)	90.06(2)
β (°)	71.243(5)	72.16(2)	72.884(18)	108.45(3)
γ (°)	83.098(4)	83.539(12)	83.906(12)	90.23(2)
V (Å^3)	369.16(4)	378.05(14)	383.35(13)	385.017(128)

Hydrogen bond tables generated from Olex2[11]

Table S6. Distances and angles of hydrogen bonds in **[fa][CH_3SO_3]**

Donor	**Proton**	**Acceptor**	**D-H (Å)**	**H···A (Å)**	**D···A (Å)**	**D-H···A(°)**
N8	H8A	O4	0.87(3)	2.05(3)	2.907(5)	167(5)
N8	H8B	O3	0.90(2)	2.54(5)	3.068(4)	118(4)
N8	H8B	O2	0.90(2)	2.25(4)	3.017(4)	143(5)
N6	H6A	O2	0.89(2)	2.04(3)	2.931(4)	174(5)
N6	H6B	O3	0.90(2)	1.94(3)	2.838(5)	177(4)
C7	H7	O3	0.93	2.37	2.999(5)	124.4
C7	H7*	O4	0.93	2.712	3.5057	143.74
Average			0.903	2.272	3.038	149.59

Table S7. Distances and angles of hydrogen bonds in **[fa][CF_3SO_3]**

Donor	**Proton**	**Acceptor**	**D-H (Å)**	**H···A (Å)**	**D···A (Å)**	**D-H···A(°)**
C1	H1	O2	0.93	2.36	3.252(5)	161.6
N2	H2A	O1	0.924(19)	1.97(2)	2.895(4)	173(4)
N2	H2B	O3	0.895(19)	2.06(2)	2.948(4)	174(4)
N1	H1A	O3	0.903(19)	2.07(3)	2.933(4)	159(5)
N1	H1B	O1	0.91(2)	2.02(2)	2.919(4)	169(6)
Average			0.9124	2.096	2.9894	167.32

Table S8. Distances and angles of hydrogen bonds in **[fa][*p*-Tos]**

Donor	**Proton**	**Acceptor**	**D-H (Å)**	**H···A (Å)**	**D···A (Å)**	**D-H···A(°)**

C1	H1	O5	0.93	2.35	3.272(2)	173
C2	H2	O2	0.93	2.31	3.183(2)	155.4
N1	H1A	O1	0.86(3)	2.04(3)	2.870(2)	163(2)
N2	H2A	O1	0.81(3)	2.01(3)	2.810(2)	173(3)
N4	H4A	O4	0.84(3)	2.00(3)	2.823(2)	168(3)
N3	H3A	O4	0.84(3)	2.04(3)	2.858(3)	167(3)
N2	H2B	O3	0.85(3)	2.12(3)	2.961(2)	178(2)
N1	H1B	O6	0.82(3)	2.09(3)	2.899(2)	173(3)
N4	H4B	O6	0.88(3)	2.04(3)	2.907(2)	172(2)
N3	H3B	O3	0.86(3)	1.99(3)	2.844(2)	173(3)
Average			0.862	2.099	2.9427	169.54

Table S9. Distances and angles of hydrogen bonds in **[fa][CF_3COO]**

Donor	**Proton**	**Acceptor**	**D-H (Å)**	**H···A (Å)**	**D···A (Å)**	**D-H···A(°)**
C9	H9	O5	0.93	2.39	3.238(3)	151.3
N10	H10A	O5	0.86(2)	2.60(3)	3.064(3)	115(3)
N10	H10A	O4	0.86(2)	2.17(3)	2.937(3)	147(3)
N10	H10B	O5	0.88(2)	2.04(2)	2.920(3)	178(3)
N8	H8A	O5	0.89(2)	2.13(2)	3.027(3)	175(3)
N8	H8B	O4	0.88(2)	2.11(2)	2.986(3)	170(4)
Average			0.883	2.39	3.0287	156.05

Table S10. Distances and angles of hydrogen bonds in **[fa]Cl**

Donor	**Proton**	**Acceptor**	**D-H (Å)**	**H···A (Å)**	**D···A (Å)**	**D-H···A(°)**
N1	H2	Cl1	0.904(17)	2.48(2)	3.268(2)	147(2)
N2	H5	Cl1	0.904(19)	2.43(2)	3.261(2)	154(4)
N1	H3	Cl1	0.900(18)	2.31(2)	3.187(2)	164(3)
N2	H4	Cl1	0.900(19)	2.32(2)	3.218(2)	176(5)
Average			0.902	2.385	3.2335	160.25
C1*	H1	Cl1	0.92(4)	2.83(4)	3.427(2)	124(2)

* *The C1 – H1 – Cl1 interaction details a H···Cl interaction that we don't consider a hydrogen bond, but is detailed here as the interaction is referred to in the text.*

Table S11. Distances and angles of hydrogen bonds in **[aca][CH_3SO_3]**

Donor	**Proton**	**Acceptor**	**D-H (Å)**	**H···A (Å)**	**D···A (Å)**	**D-H···A(°)**
N1	H1A	O1	0.90(2)	2.13(2)	3.0209(19)	170(3)
N1	H1B	O2	0.90(2)	1.98(2)	2.873(2)	171(3)
Average			0.90	2.06	2.95	170.5

Table S12. Distances and angles of hydrogen bonds in **[aca][CF_3SO_3]**

Donor	Proton	Acceptor	D-H (Å)	H···A (Å)	D···A (Å)	D-H···A(°)
N1	H1A	O2	0.882(19)	2.04(2)	2.917(4)	171(4)
N4	H4A	O4	0.886(19)	2.02(2)	2.903(4)	175(4)
N4	H4B	O5	0.895(19)	2.020(19)	2.913(4)	176(3)
N1	H1B	O1	0.884(19)	2.037(19)	2.921(4)	177(4)
N3	H3A	O4	0.914(19)	2.04(2)	2.944(4)	172(4)
N2	H2A	O2	0.898(19)	2.04(2)	2.930(4)	171(4)
N3	H3B	O3	0.91(2)	2.00(2)	2.901(4)	171(5)
N2	H2B	O6	0.901(19)	2.04(2)	2.931(4)	172(4)
Average			0.90	2.03	2.92	173.13

Table S13. Distances and angles of hydrogen bonds in **[aca][*p*-Tos]**

Donor	Proton	Acceptor	D-H (Å)	H···A (Å)	D···A (Å)	D-H···A(°)
N1	H1A	O3	0.876(18)	2.00(2)	2.845(3)	163(3)
N1	H1B	O2	0.878(18)	2.025(19)	2.895(3)	170(3)
N2	H2A	O3	0.905(19)	1.93(2)	2.820(3)	166(3)
N2	H2B	O1	0.904(18)	1.95(2)	2.815(3)	159(3)
Average			0.89	1.98	2.84	164.5

Table S14. Distances and angles of hydrogen bonds in **[aca][CF3COO]**

Donor	Proton	Acceptor	D-H (Å)	H···A (Å)	D···A (Å)	D-H···A(°)
N1	H1A	O5	0.898(18)	2.021(19)	2.916(3)	174(3)
N1	H1B	O8	0.893(19)	2.01(2)	2.887(3)	166(4)
N2	H2A	O6	0.903(18)	1.979(19)	2.879(3)	174(3)
N2	H2B	O3	0.884(18)	2.02(2)	2.884(3)	164(3)
N3	H3A	O4	0.893(19)	1.98(2)	2.865(3)	173(4)
N3	H3B	O2	0.912(19)	1.923(19)	2.831(3)	173(4)
N4	H4A	O3	0.903(19)	2.03(2)	2.930(3)	174(4)
N4	H4B	O5	0.898(19)	1.95(2)	2.835(3)	170(4)
N5	H5A	O1	0.902(19)	1.96(2)	2.858(3)	171(3)
N5	H5B	O4	0.898(18)	1.98(2)	2.802(3)	152(3)
N6	H6A	O2	0.902(19)	1.944(19)	2.842(3)	174(4)
N6	H6B	O7	0.902(19)	1.95(2)	2.805(3)	157(4)
N7	H7A	O7	0.910(18)	1.931(19)	2.839(3)	175(3)
N7	H7B	O6	0.903(18)	1.94(2)	2.799(3)	158(4)
N8	H8D	O1	0.893(18)	1.98(2)	2.863(3)	168(3)
N8	H8E	O8	0.894(18)	2.08(2)	2.965(3)	170(3)

Average	0.90	1.98	2.86	168.31

Hydrogen bond tables of structures from the literature, with distances and angles calculated through the Mercury 3.8 software[12]

Table S15. Distances and angles of hydrogen bonds in **[aca]Cl**

Donor	Proton	Acceptor	D-H (Å)	H···A (Å)	D···A (Å)	D-H···A(°)
N1	H1A	Cl	0.836	2.496	3.266	153.48
N1	H1B	Cl	0.836	2.356	3.190	176.24
N2	H2B	Cl	0.846	2.426	3.209	154.26
N2	H2A	Cl	0.809	2.386	3.194	177.27
Average			0.832	2.416	3.21	165.3

Table S16. Distances and angles of hydrogen bonds in **[gdm][CH_3SO_3]**

Donor	Proton	Acceptor	D-H (Å)	H···A (Å)	D···A (Å)	D-H···A(°)
N2	H2N	O2	0.848	2.077	2.913	168.24
N1	H1N	O1	0.793	2.126	2.909	169.39
N2	H3N	O1	0.798	2.139	2.925	168.39
Average			0.81	2.11	2.92	168.67

Table S17. Distances and angles of hydrogen bonds in **[gdm][CF_3SO_3]**

Donor	Proton	Acceptor	D-H (Å)	H···A (Å)	D···A (Å)	D-H···A(°)
N1	H1	O2	0.81	2.192	3	175.35
N3	H6	O3	0.84	2.161	2.997	173.19
N3	H5	O1	0.906	2.092	2.997	170.65
N2	H4	O2	0.801	2.2	2.993	170.42
N1	H2	O1	0.891	2.092	2.981	174.89
N2	H3	O3	0.834	2.155	2.985	173.6
Average			0.85	2.15	2.99	173.02

Table S18. Distances and angles of hydrogen bonds in **[gdm][*p*-Tos]**

Donor	Proton	Acceptor	D-H (Å)	H···A (Å)	D···A (Å)	D-H···A(°)
N4	H22	O6	1.009	1.871	2.876	173.39
N1	H1N	O5	1.009	1.894	2.886	166.77
N2	H3N	O3	1.009	1.901	2.894	167.52
N1	H18	O3	1.009	1.915	2.922	175.82
N6	H25	O1	1.008	1.918	2.923	174.52
N2	H17	O6	1.009	1.936	2.908	160.75
N3	H20	O1	1.009	1.943	2.94	169.36

N1	H16	O5	1.01	1.956	2.933	162.03
N5	H24	O2	1.009	1.97	2.949	162.75
N3	H19	O2	1.009	1.989	2.955	159.17
N6	H26	O4	1.009	1.994	2.958	158.72
N5	H23	O4	1.009	2.037	3.011	161.46
Average			1.01	1.94	2.93	166.02

Table S19. Distances and angles of hydrogen bonds in **[gdm][CF_3COO]**

Donor	**Proton**	**Acceptor**	**D-H (Å)**	**H···A (Å)**	**D···A (Å)**	**D-H···A(°)**
N2	H3	O2	0.86	2.084	2.943	175.62
N3	H5	O1	0.86	2.131	2.959	161.59
N2	H4	O1	0.86	2.405	3.148	145.01
N1	H1	O1	0.859	2.215	2.999	151.6
N3	H6	O2	0.86	2.295	3.081	152.02
N1	H2	O2	0.86	2.389	3.122	145.12
Average			0.86	2.25	3.04	155.16

Hirshfeld surfaces interactions breakdown

Table S20. Breakdown of interactions calculated from the Hirshfeld surfaces of the [CH_3SO_3] salts, for both the ion pair and individual ions

[CH_3SO_3]	**[gdm]**	**[aca]**	**[fa]**
Reciprocals			
H-O %	44.3	44.5	57.1
H-H %	43.3	46.4	32.3
H-C %	1	2.8	2.2
H-S %	0.1	0.2	0.1
H-N %	7.9	5.8	5
From cation			
H-O %	41.5	37.7	40.4
H-H %	42.3	51.1	45.1
H-C %	0	1	0
H-S %	1.2	0.2	0.2
H-N %	0.1	1.4	0.8
From anion			
H-O %	6.8	8.4	12
H-H %	34.4	28.4	24.8
H-C %	0	1.5	1.4
H-S %	0	0	0
H-N %	2.6	2.5	2.4
O-H %	54.3	58.2	57.1

Table S21. Breakdown of interactions calculated from the Hirshfeld surfaces of the [CF_3SO_3] salts, for both the ion pair and individual ions

[CF_3SO_3]	**[gdm]**	**[aca]**	**[fa]**
Reciprocals			
H-O %	35.8	37.4	42.2
H-H %	10	13.2	5.4
H-C %	3.8	0.3	0.2
H-S %	0.3	0.1	0.3
H-N %	0.2	1.6	1.3
H-F %	22.5	23.5	18.9
From cation			
H-O %	44.4	45.3	51.6
H-H %	16.9	21.3	11.5
H-C %	0.4	0.1	0.5
H-S %	0.2	0	0.3
H-N %	6.1	1	2.8
H-F %	21.6	23.5	23.8
From anion			
O-H %	43.5	46	42.1
F-H %	20.9	22.76	17.7

Table S22. Breakdown of interactions calculated from the Hirshfeld surfaces of the [*p*-Tos] salts, for both the ion pair and individual ions

[*p*-Tos]	**[gdm]**	**[aca]**	**[fa]**
Reciprocals			
H-O %	31.9	31.8	33.5
H-H %	41.7	46.8	40.7
H-C %	17.7	16	19
H-S %	0.1	0.2	0
H-N %	6.1	3.2	3.8
From cation			
H-O %	44.9	31.8	50
H-H %	37.5	50.4	34.6
H-C %	0.3	0	0.4
H-S %	0.1	0.3	0.2
H-N %	2.8	1.3	5.2
From anion			
H-O %	3.2	3.7	2.8
H-H %	38.2	40.2	39.9
H-C %	10.5	10.4	10.4
H-S %	0	0	0
H-N %	1.9	0.9	1.1
C-H %	10.4	11.5	12

Table S23. Breakdown of interactions calculated from the Hirshfeld surfaces of the [CF_3COO] salts, for both the ion pair and individual ions

[CF_3COO]	**[gdm]**	**[aca]**	**[fa]**
Reciprocals			
H-O %	21.9	25	36.3
H-H %	13.6	17.7	9.8
H-C %	0.9	2	0.6
H-S %	-	-	-
H-N %	0.8	3.5	0.4
H-F %	37.6	33.2	28.8
From cation			
H-O %	29.2	30.2	32.9
H-H %	23.1	23.8	19.8
H-C %	0.3	1.8	0
H-S %	-	-	0
H-N %	1.5	2.1	0.9
H-F %	31.6	33.4	32.4
From anion			
O-H %	33.6	36.7	33.5
F-H %	34.5	37.5	31.6

Table S24. Breakdown of interactions calculated from the Hirshfeld surfaces of the chloride salts, for both the ion pair and individual ions

Cl	**[aca]**	**[fa]**
Reciprocals		
H-Cl %	35.9	37.8
H-H %	51.5	36.7
H-C %	4.1	3.9
H-N %	8.6	9.4
From cation		
H-Cl %	24.6	30.5
H-H %	59.5	49.2
H-C %	2.5	1.7
H-N %	4.7	5.7
From anion		
Cl-H %	100	97.1
Cl-C %	0	2.1
Cl-N	0	0.8

DSC data

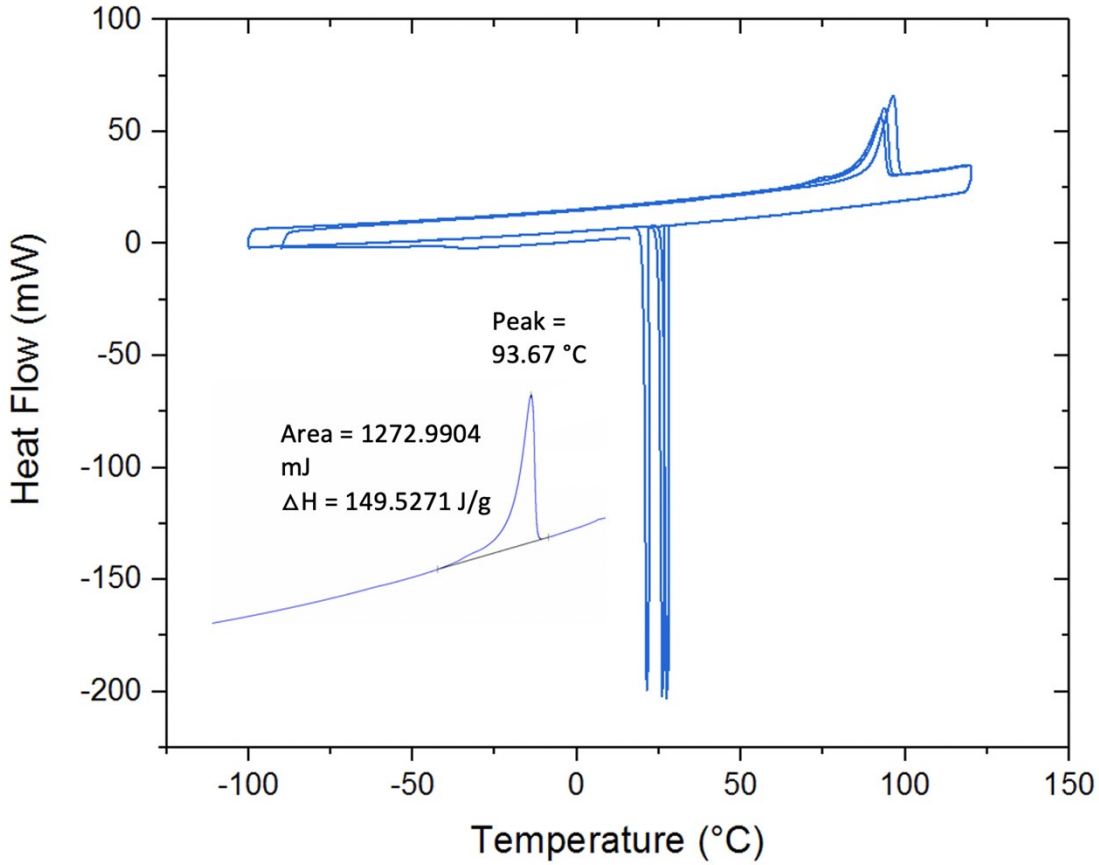

Figure S22. DSC curve of [fa][CH_3SO_3]. The melting transition from the second heating cycle is shown in purple, with thermal properties highlighted.

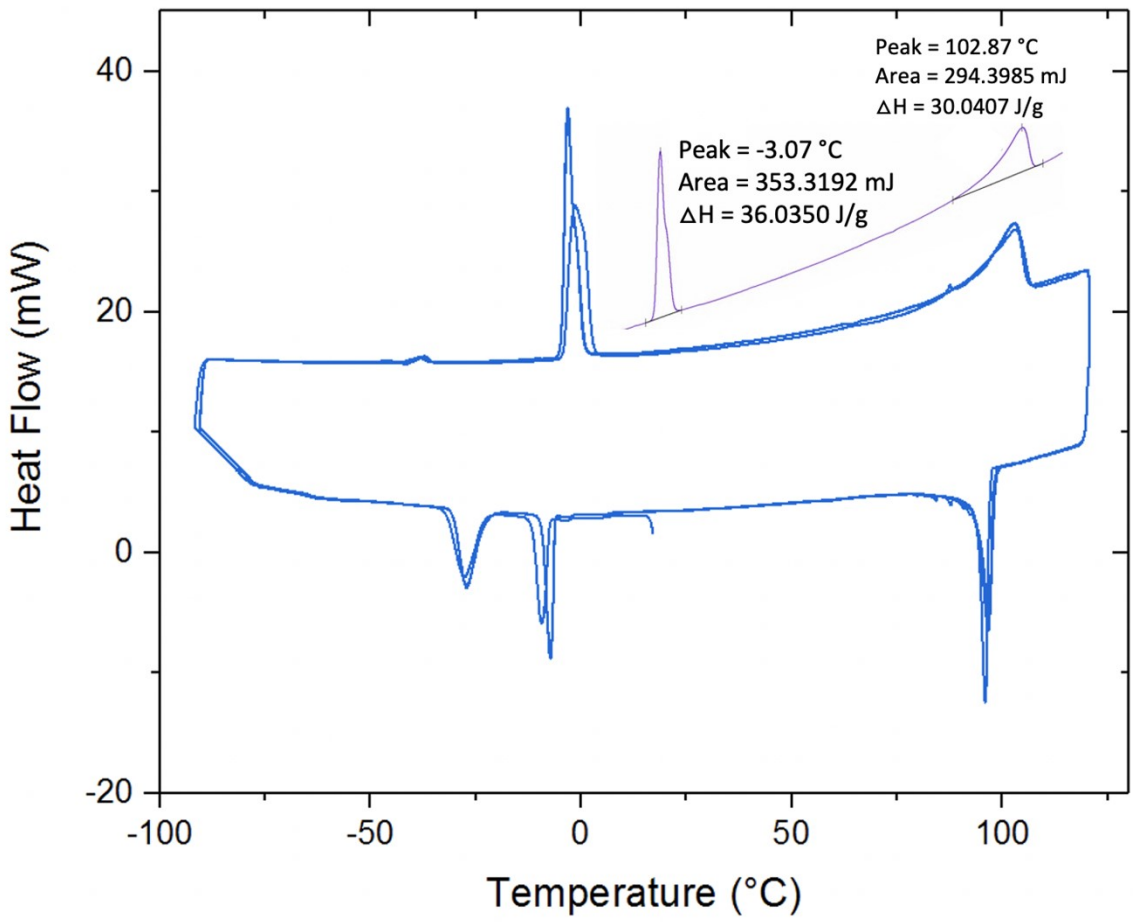

Figure S23. DSC curve of [fa][CF_3SO_3]. The relevant transitions from the second heating cycle are shown in purple, with thermal properties highlighted.

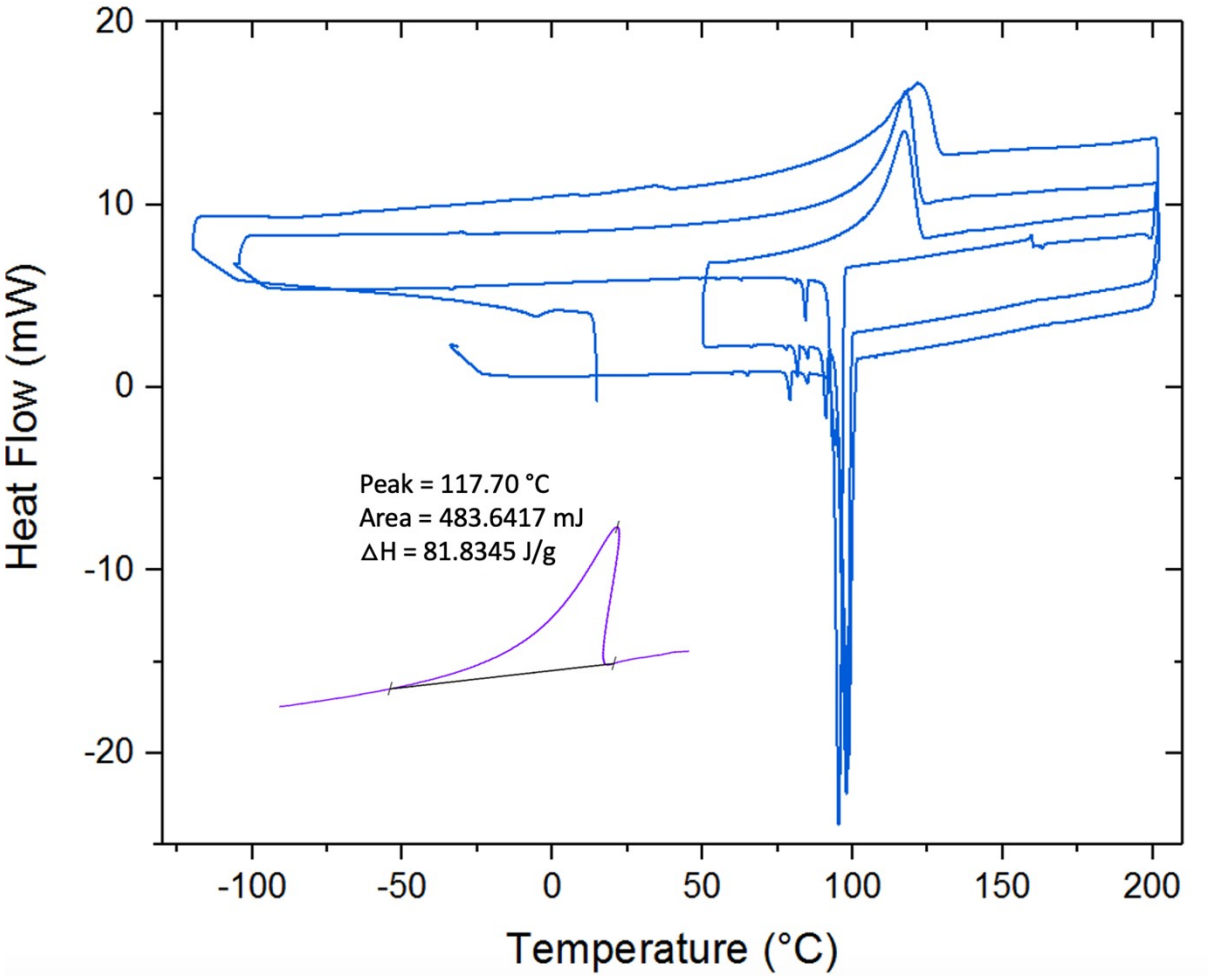

Figure S24. DSC curve of [fa][*p*-Tos]. The melting transition from the second heating cycle is shown in purple, with thermal properties highlighted.

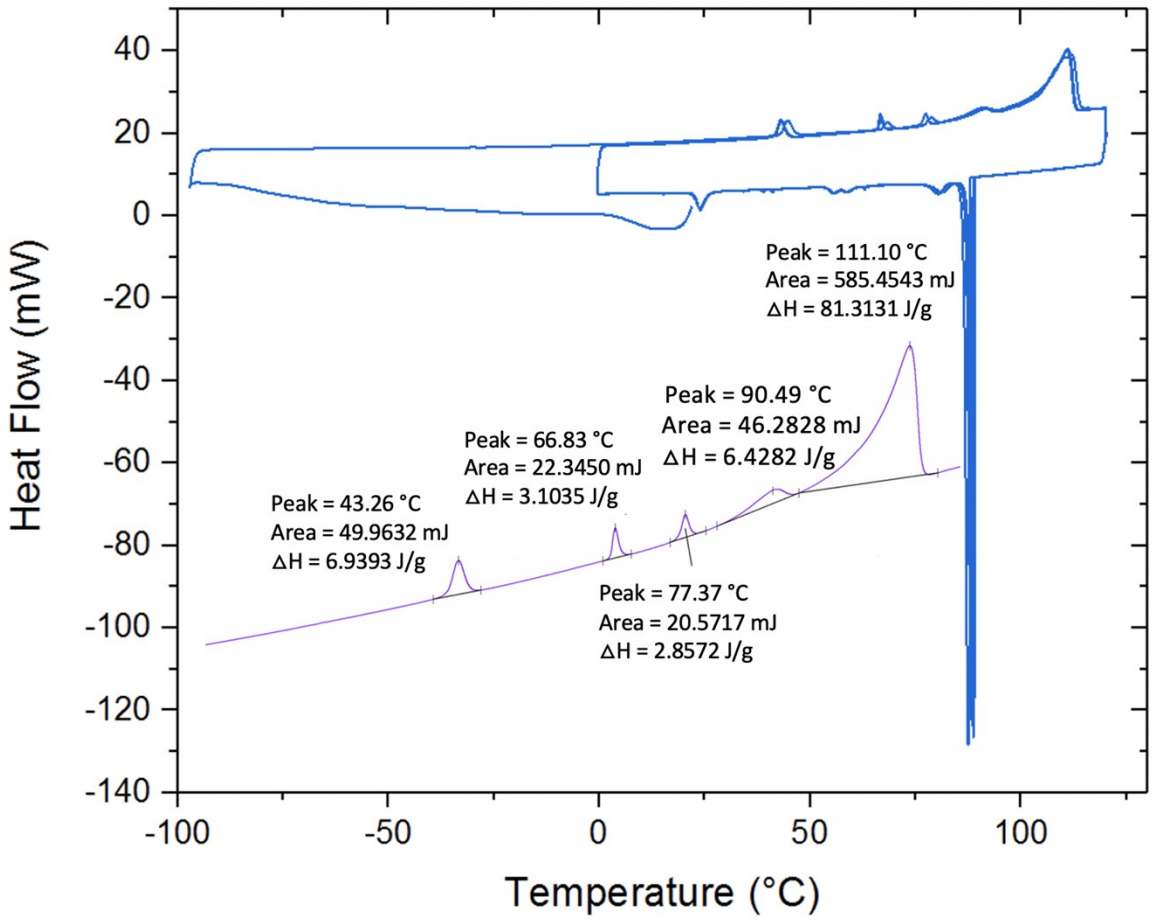

Figure S25. DSC curve of [fa][CF_3COO]. The relevant transitions from the second heating cycle are shown in purple, with thermal properties highlighted.

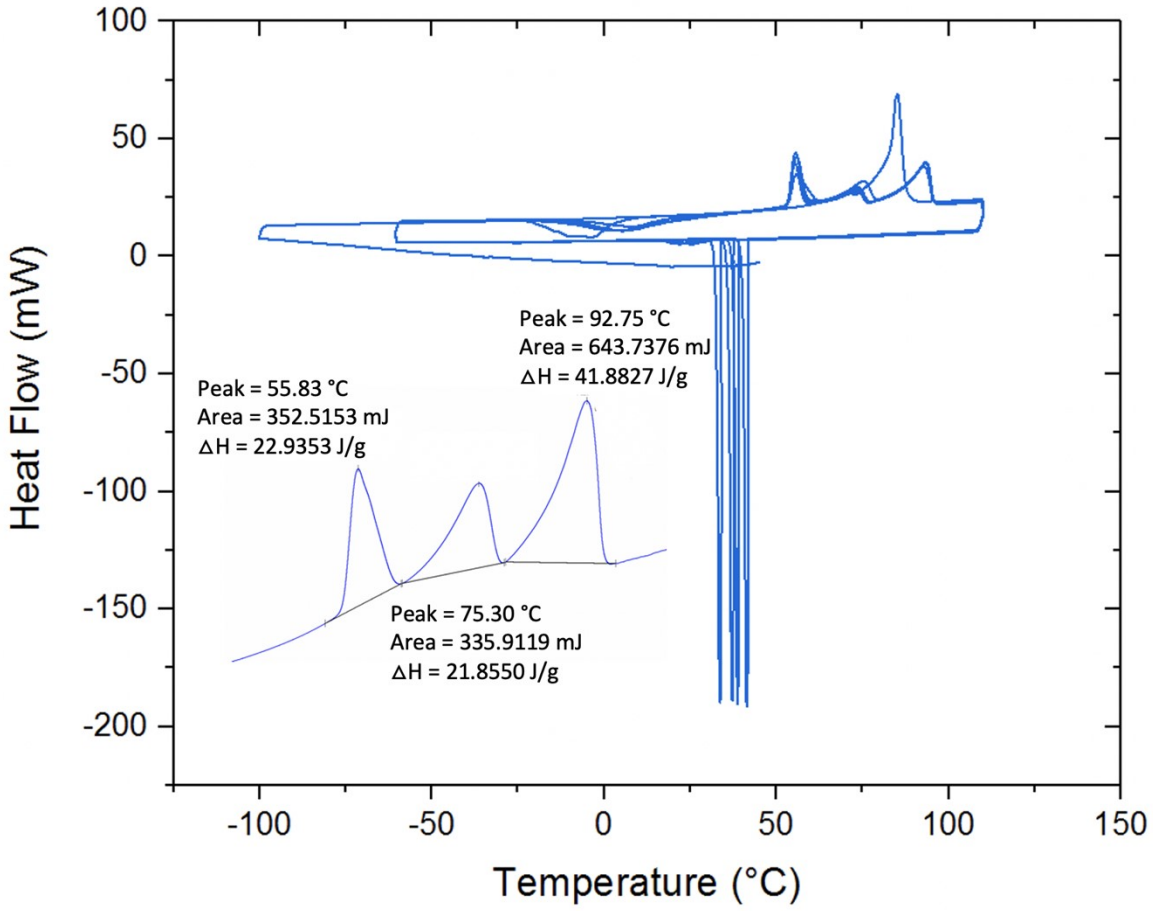

Figure S26. DSC curve of [fa]Cl. The relevant transitions from the second heating cycle are shown in purple, with thermal properties highlighted.

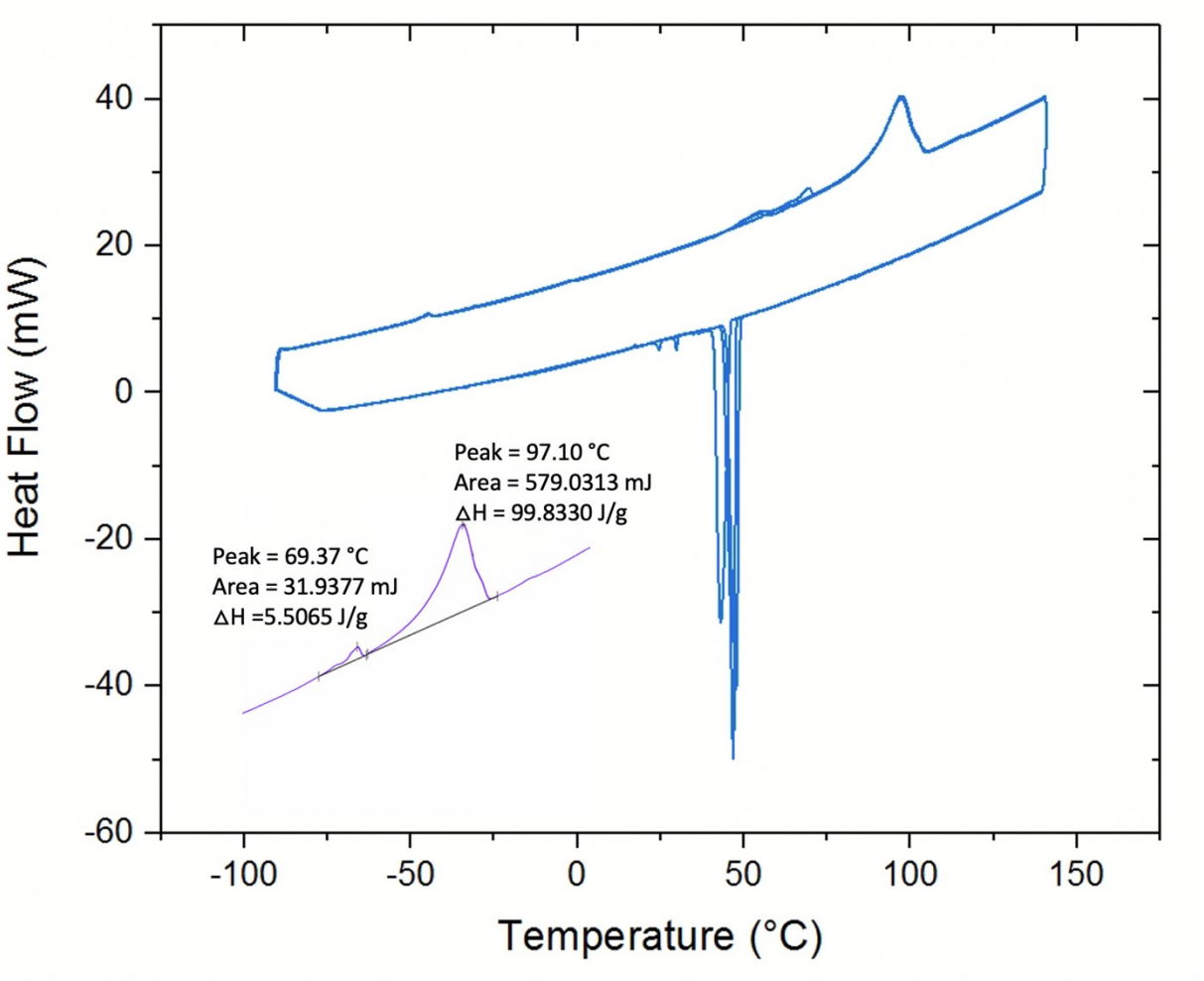

Figure S27. DSC curve of [aca][CH_3SO_3]. Transitions from the second heating cycle are shown in purple, with thermal properties highlighted. The solid-solid transition(s) are not consistently observed and so are omitted from discussion in the main text.

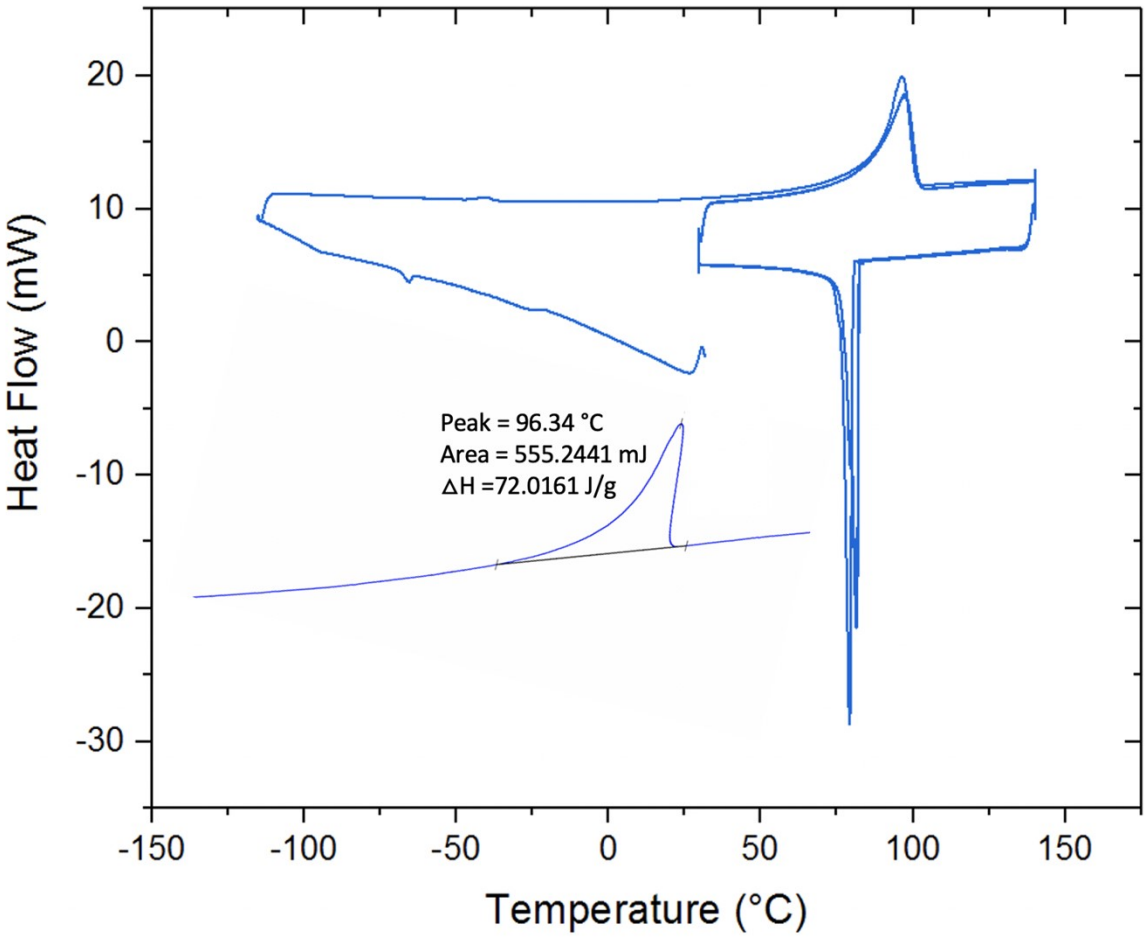

Figure S28. DSC curve of [aca][CF_3SO_3]. The melting transition from the second heating cycle is shown in purple, with thermal properties highlighted.

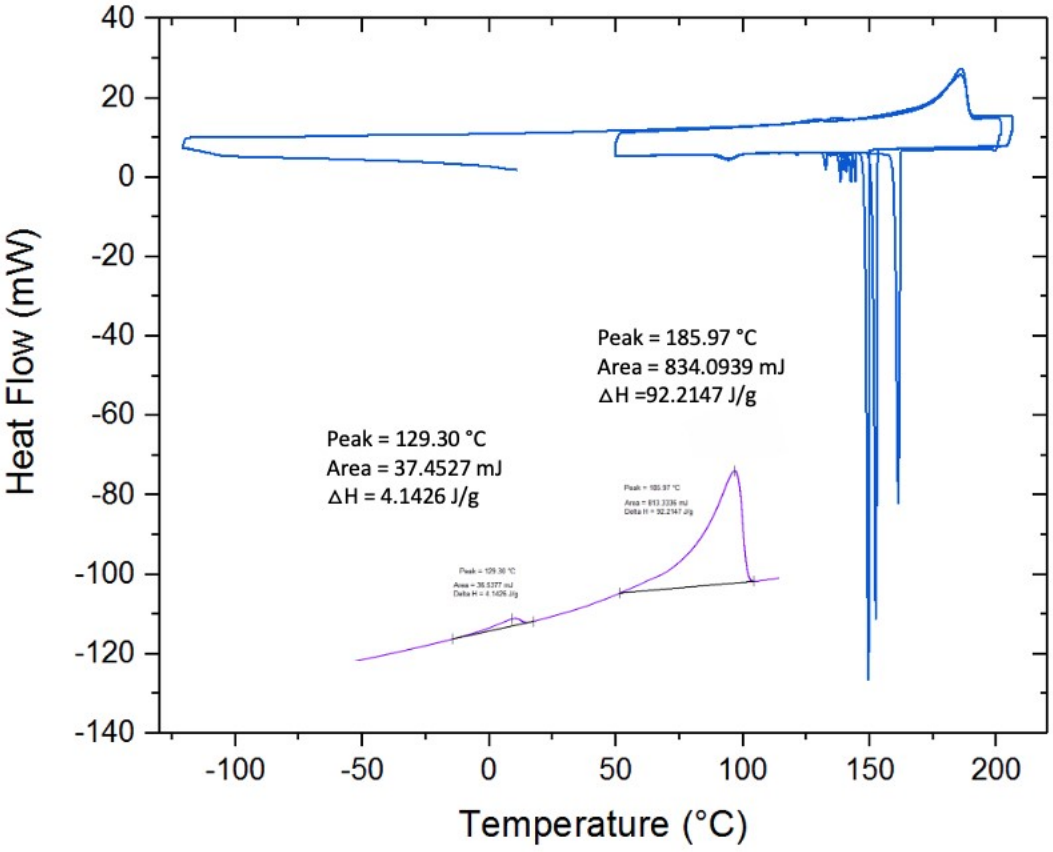

Figure S29. DSC curve of [aca][*p*-Tos]. The relevant transitions from the second heating cycle are shown in purple, with thermal properties highlighted.

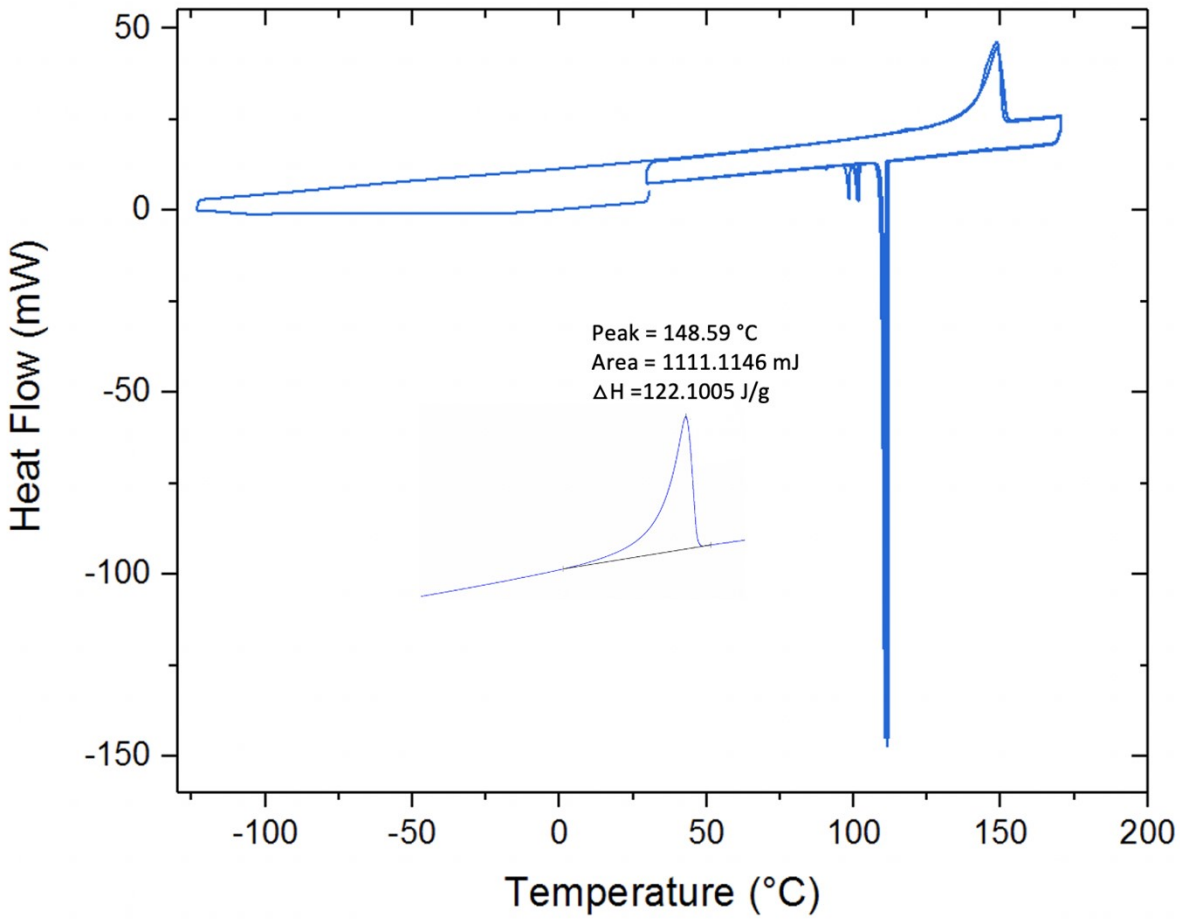

Figure S30. DSC curve of [aca][CF_3COO]. The melting transition from the second heating cycle is shown in purple, with thermal properties highlighted.

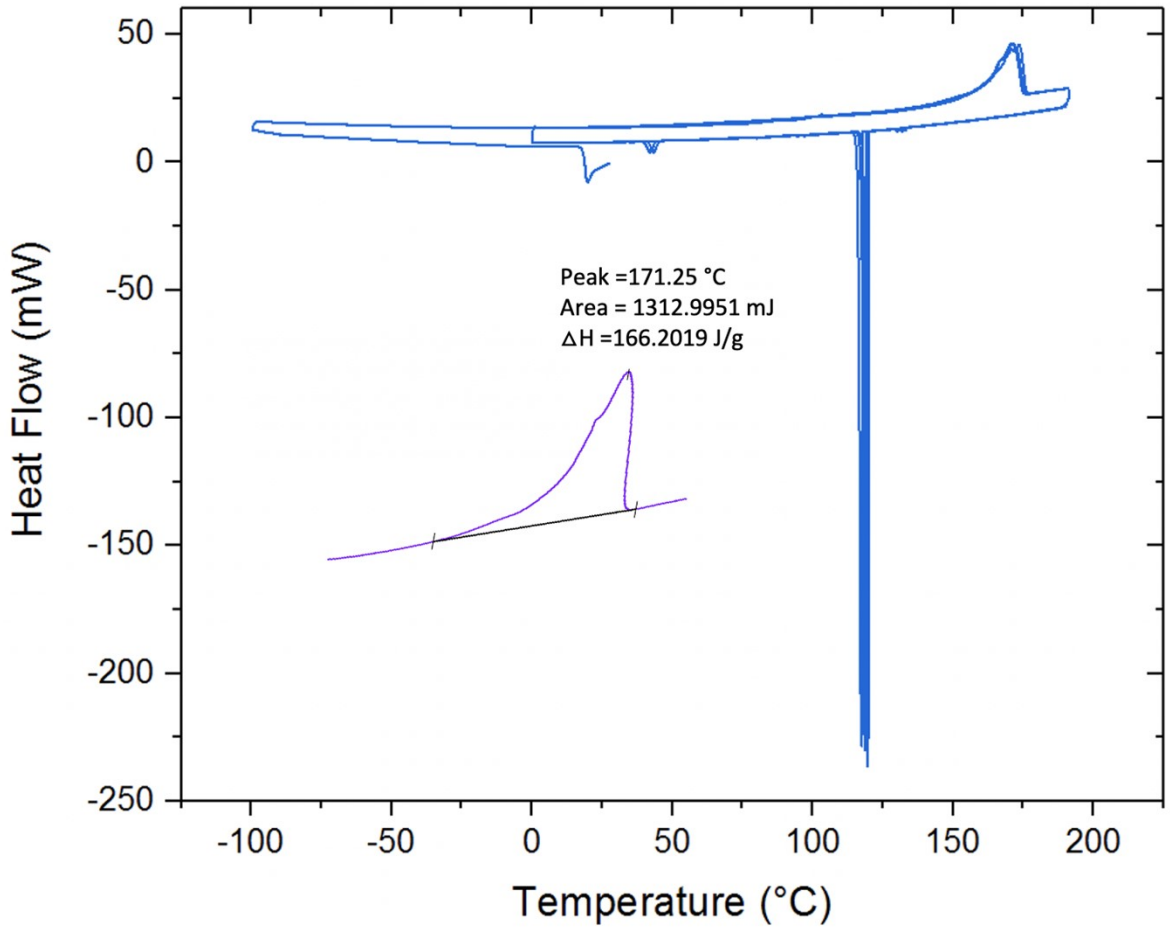

Figure S31. DSC curve of [aca]Cl. The melting transition from the second heating cycle is shown in purple, with thermal properties highlighted.

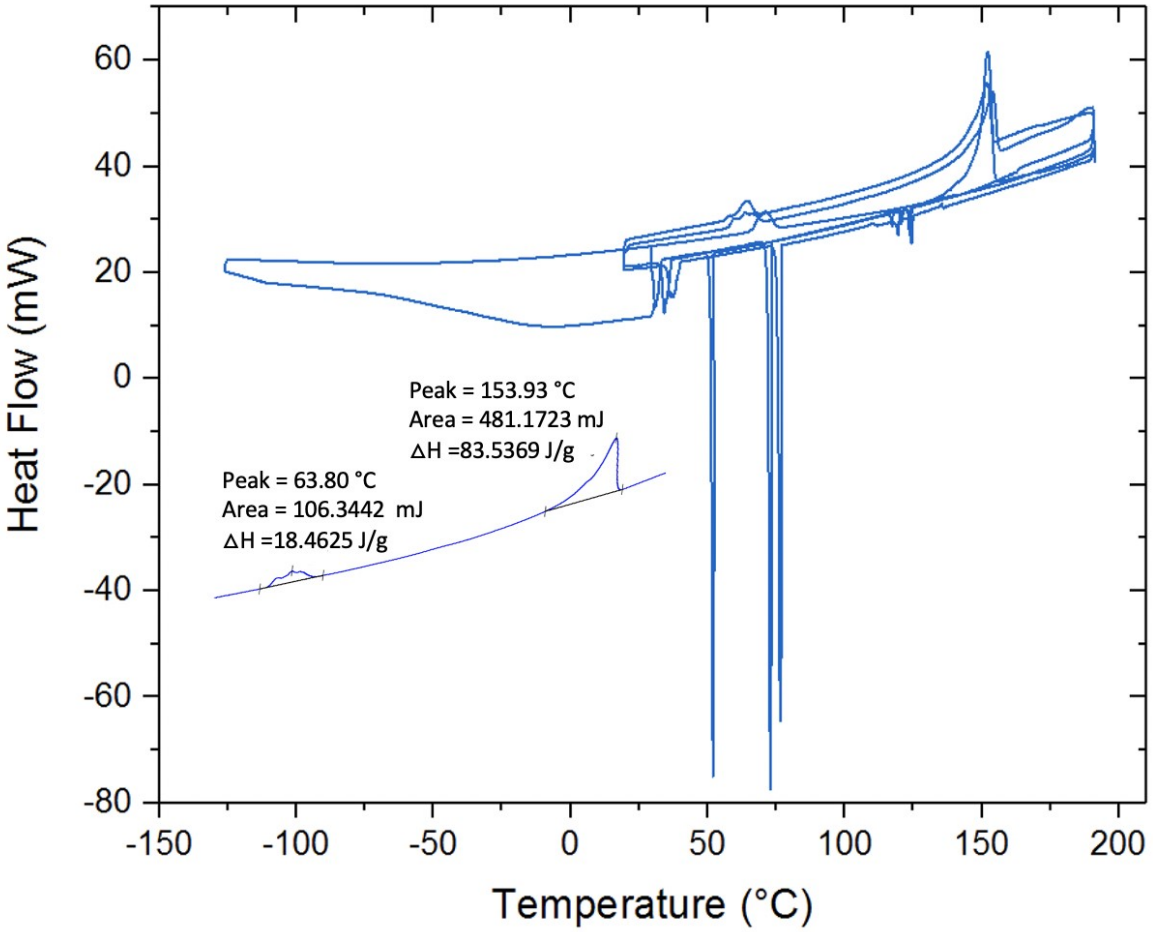

Figure S32. DSC curve of [gdm][CF_3COO]. The relevant transitions from the second heating cycle are shown in purple, with thermal properties highlighted.

Input data for Figure 7b

Table S24. Enthalpy of fusion (ΔH_f), entropy of fusion (ΔS_f) and degree of disorder introduced upon melting as calculated with the Boltzmann Equation

Material	ΔH_f kJ/mol	ΔS_f J/mol/K	Degree of disorder
[gdm][CH_3SO_3]	29	60	1362
[fa][CH_3SO_3]	21	57	949
[aca][CH_3SO_3]	15.4	42	156
[gdm][CF_3SO_3]	27	62	1732
[fa][CF_3SO_3]	5.8	16	7
[aca][CF_3SO_3]	14.8	41	139
[gdm][p-Tos]	21	42	156
[fa][p-Tos]	17.7	45	224
[aca][p-Tos]	21.2	49	362
[gdm][CF_3COO]	14.4	34	60
[fa][CF_3COO]	12.8	33	53

[aca][CF_3COO]	21	50	409
[fa]Cl	3.4	9.2	3
[aca]Cl	15.7	35	7

Degree of introduced disorder was calculated by rearranging the Boltzmann equation:

$$\Delta S_f = R \ln(N)$$

to give:

$$N = e^{\frac{\Delta Sf}{R}}$$

Where R is the ideal gas constant and N describes the ratio of number of possible arrangements/conformations in the liquid state over the number of possible arrangements/confirmations per molecule in the solid-phase.[13] This gives the data in Table S24 that is the data input into Figure S7b.

NMR Spectra of synthesised compounds

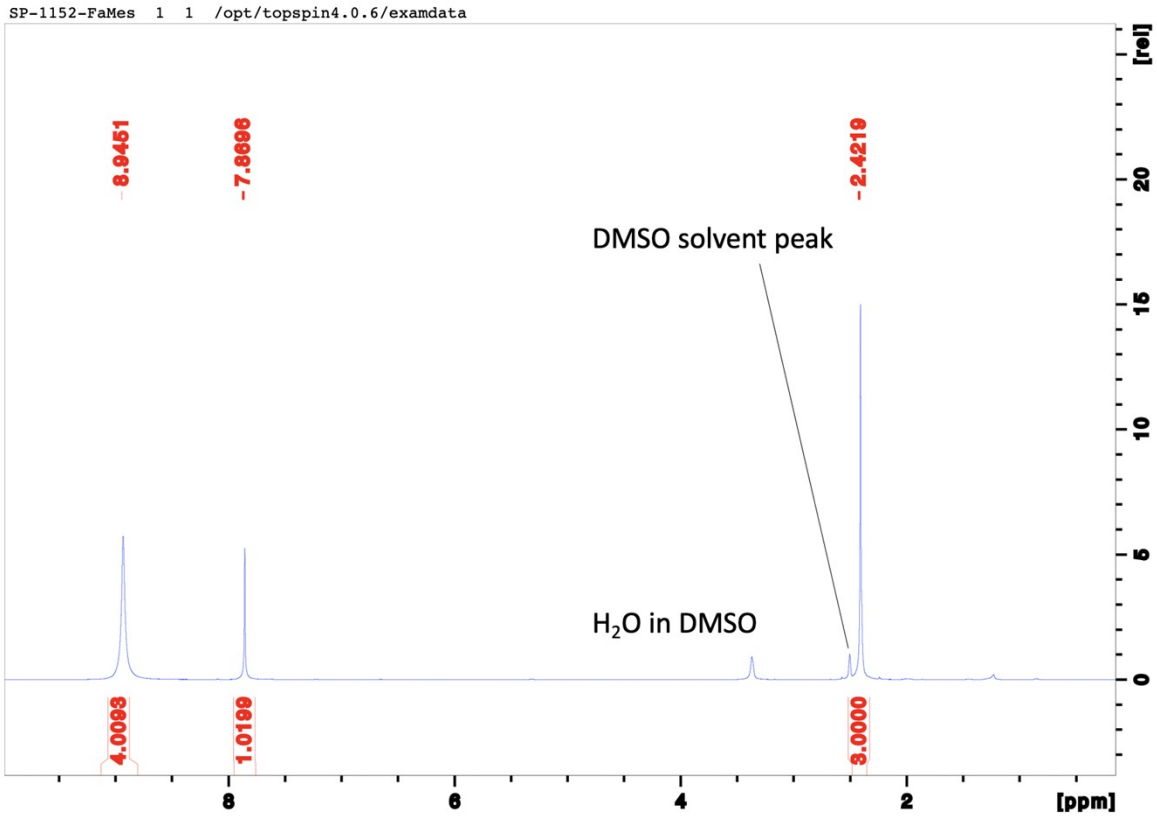

Figure S33. ^{1}H NMR spectrum of [fa][CH_3SO_3]

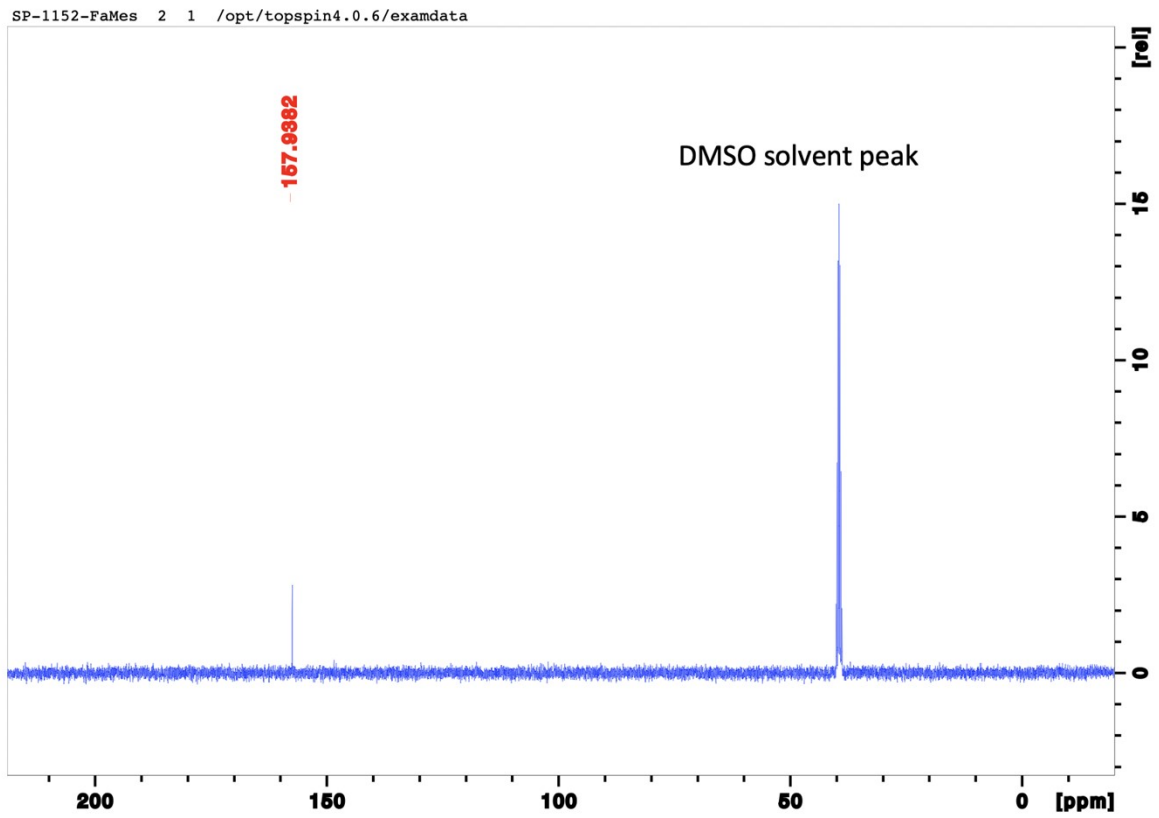

Figure S34. ^{13}C NMR spectrum of [fa][CH_3SO_3]

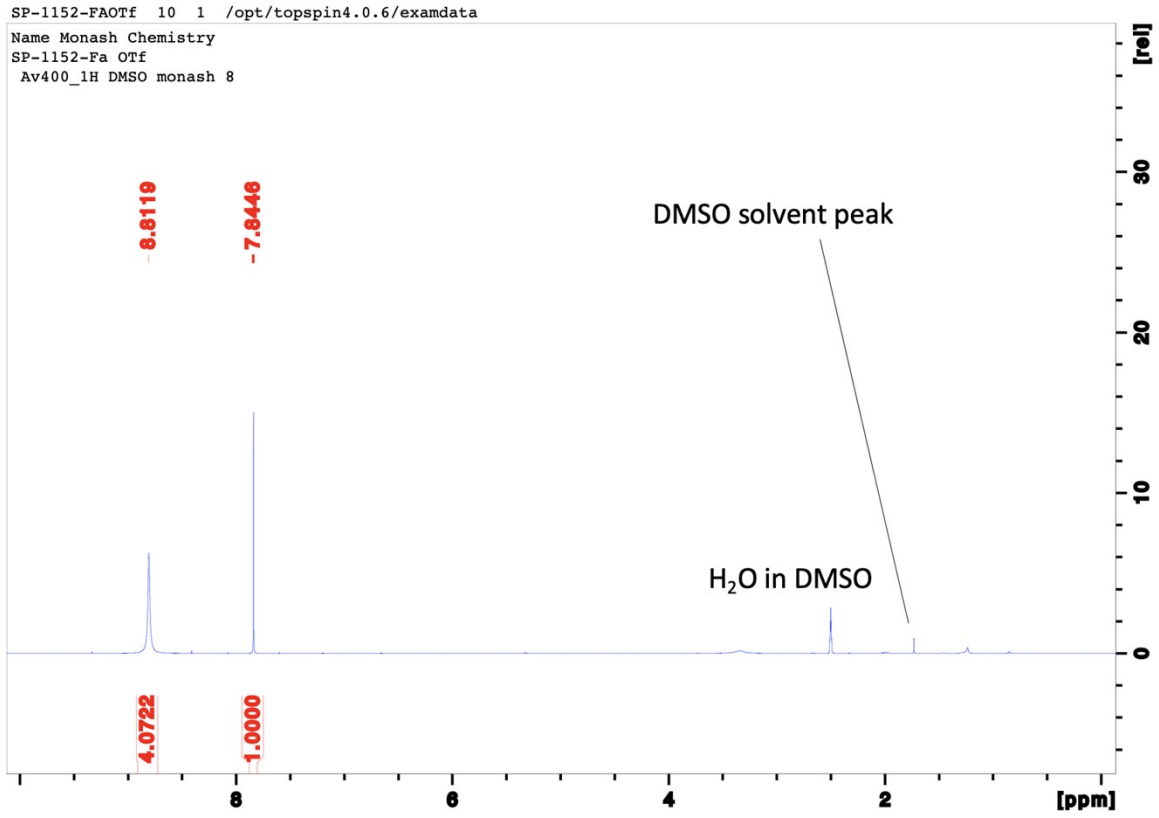

Figure S35. ^{1}H NMR spectrum of [fa][CF_3SO_3]

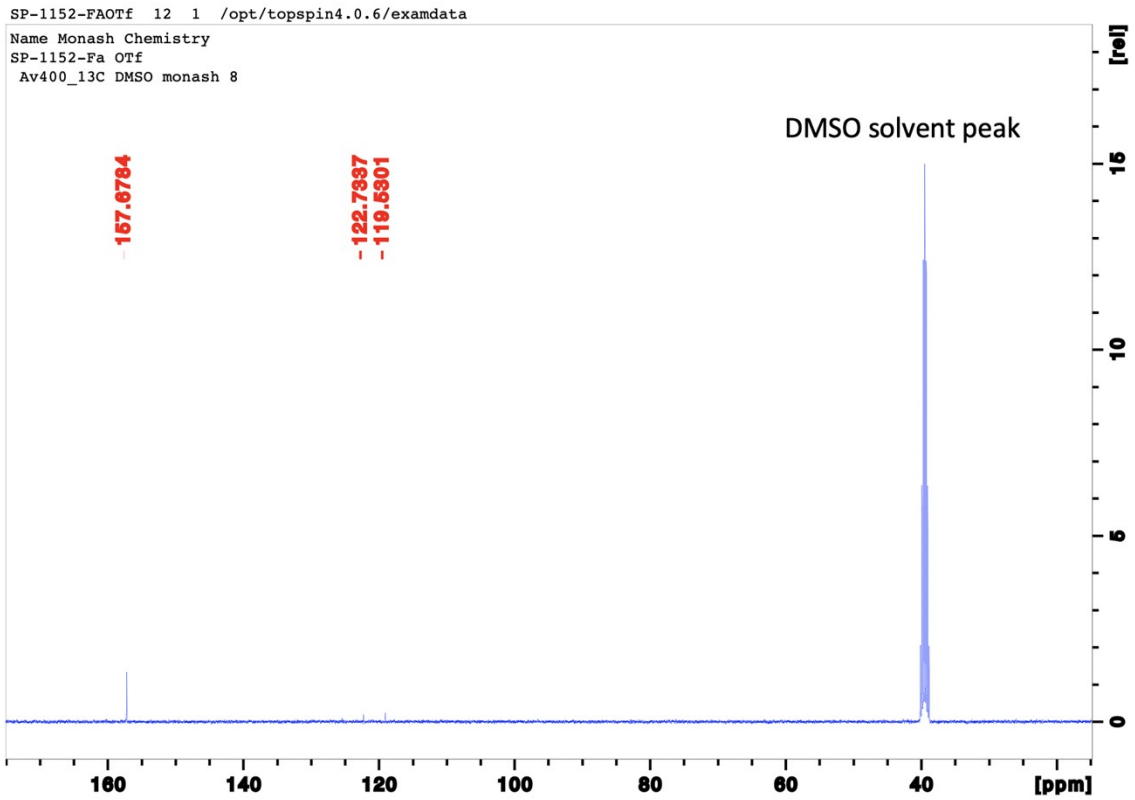

Figure S36. ^{13}C NMR spectrum of [fa][CF_3SO_3]

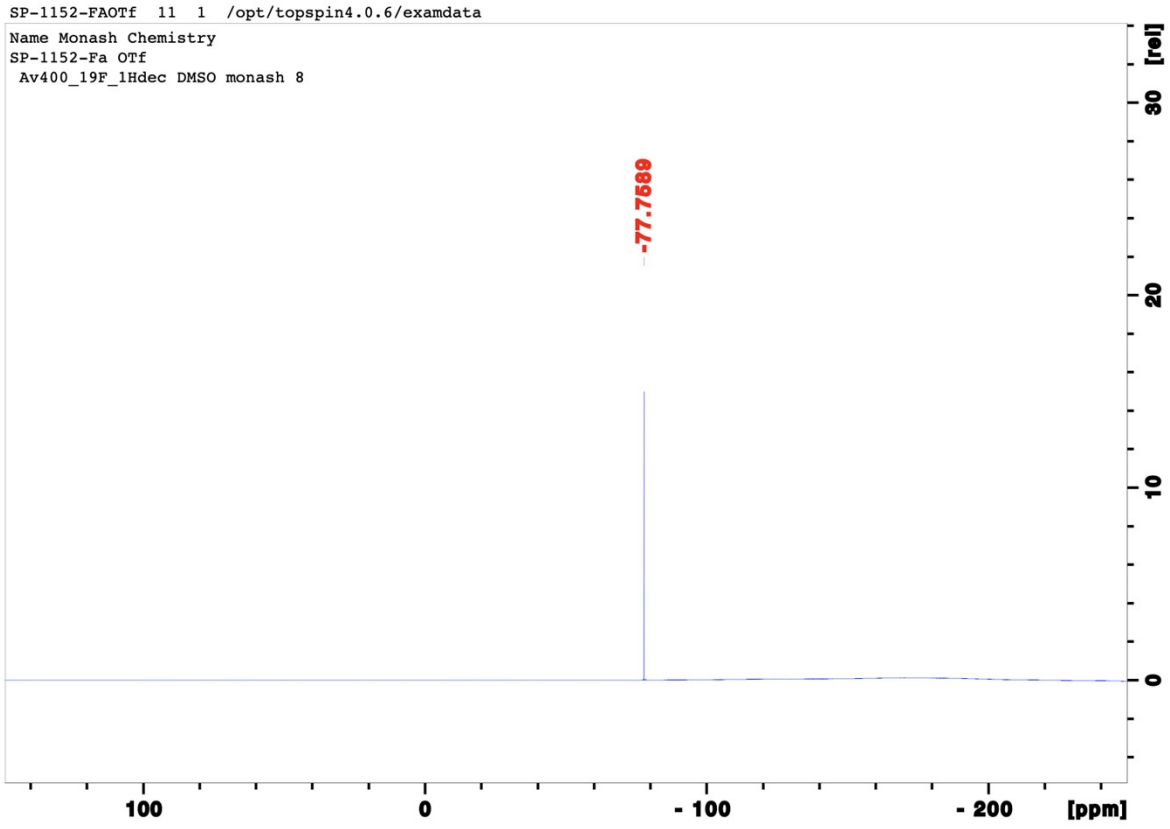

Figure S37. ^{19}F NMR spectrum of [fa][CF_3SO_3]

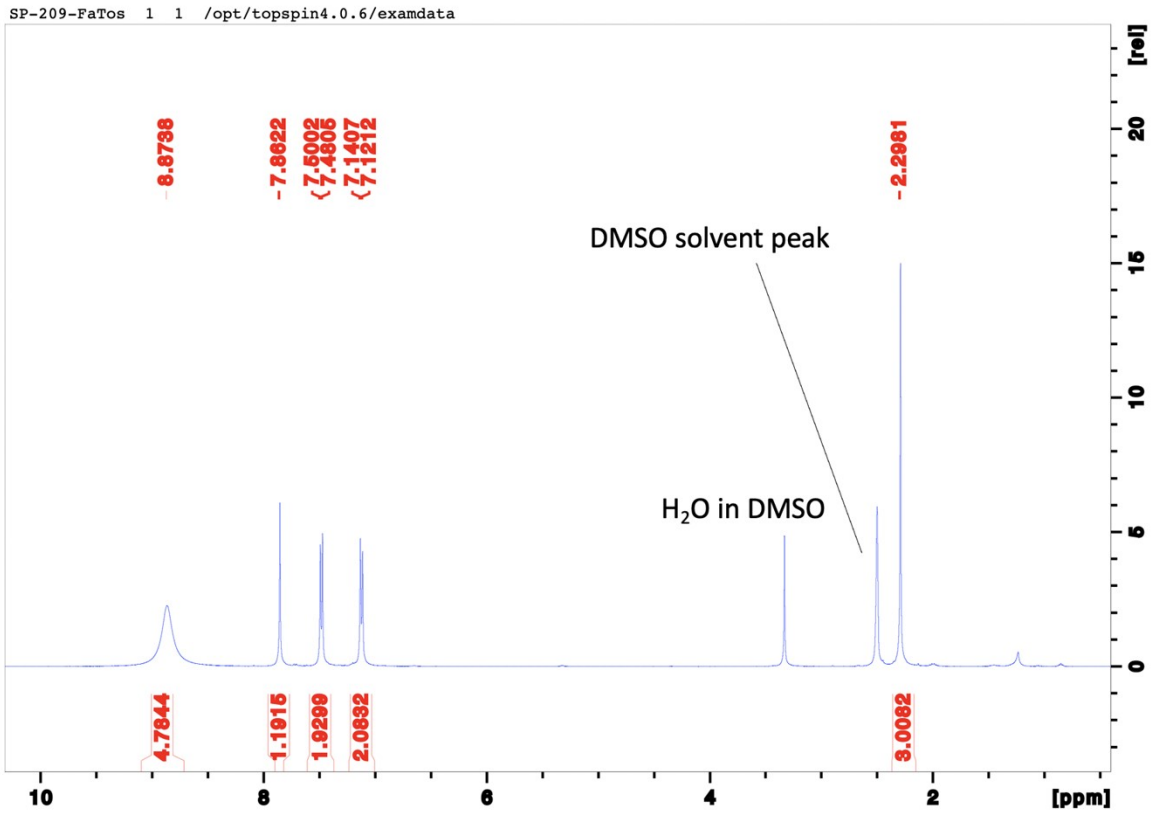

Figure S38. ^{1}H NMR spectrum of [fa][*p*-Tos]

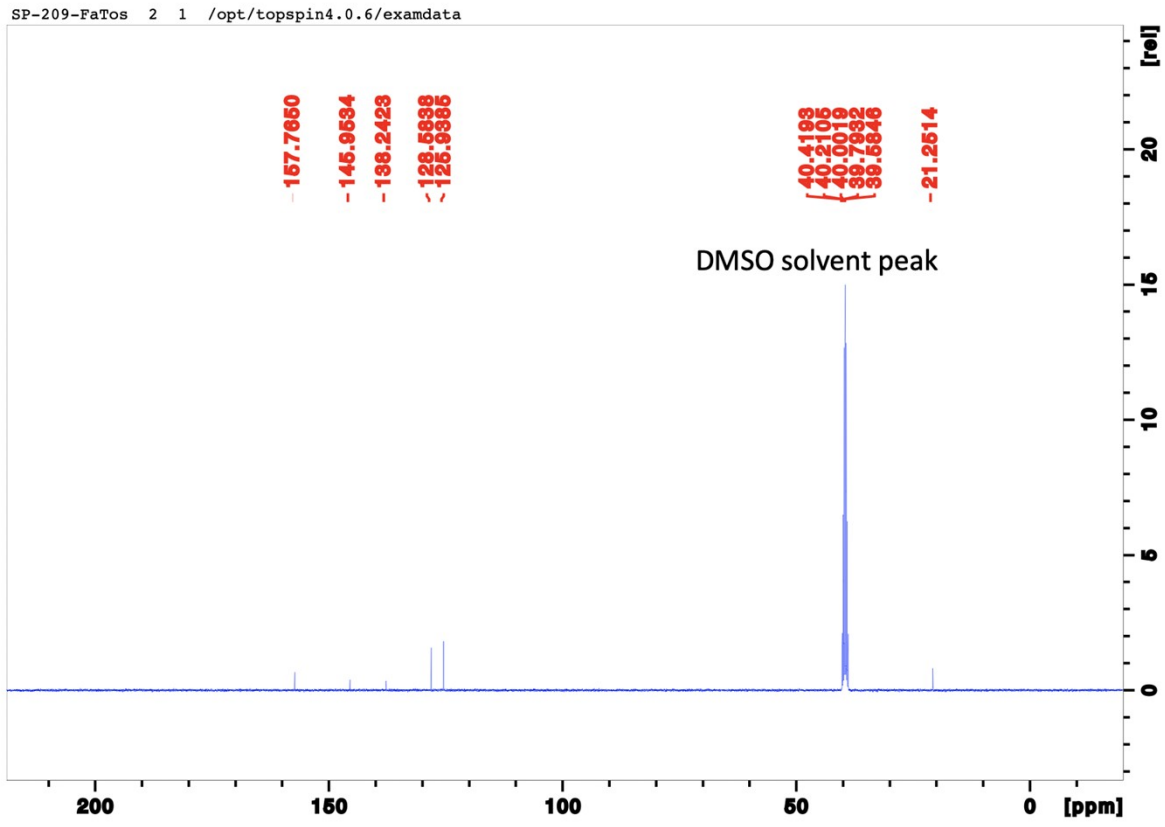

Figure S39. ^{13}C NMR spectrum of [fa][*p*-Tos]

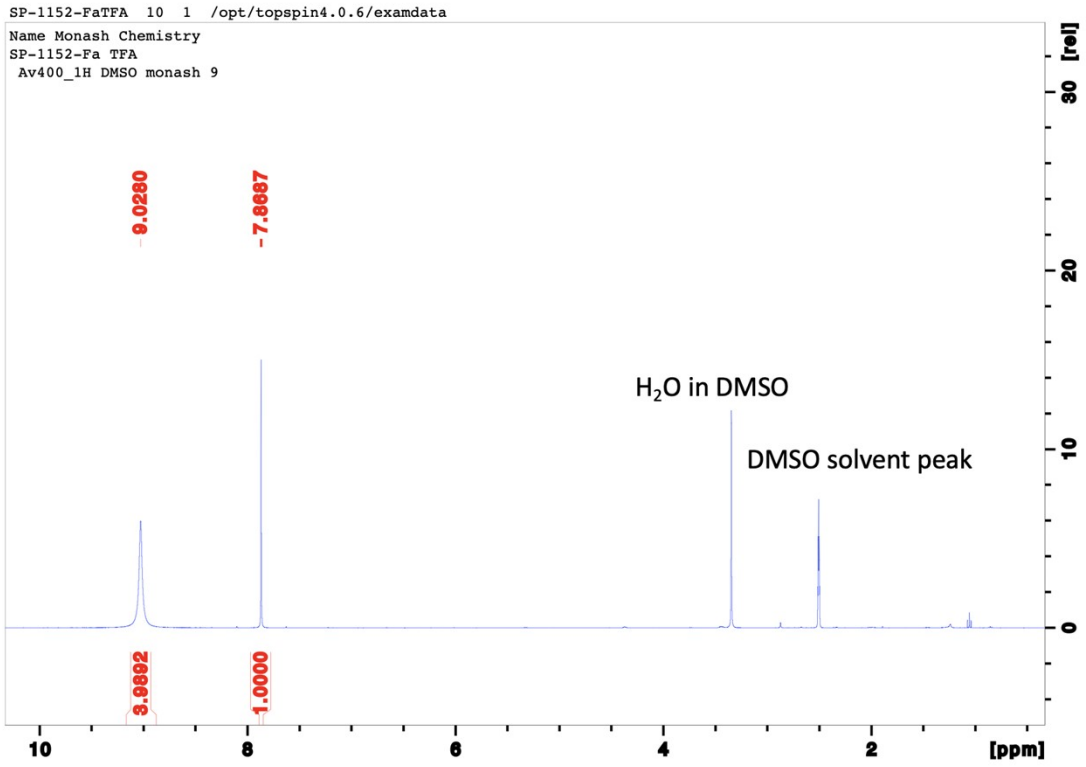

Figure S40. ^{1}H NMR spectrum of [fa][CF_3COO]

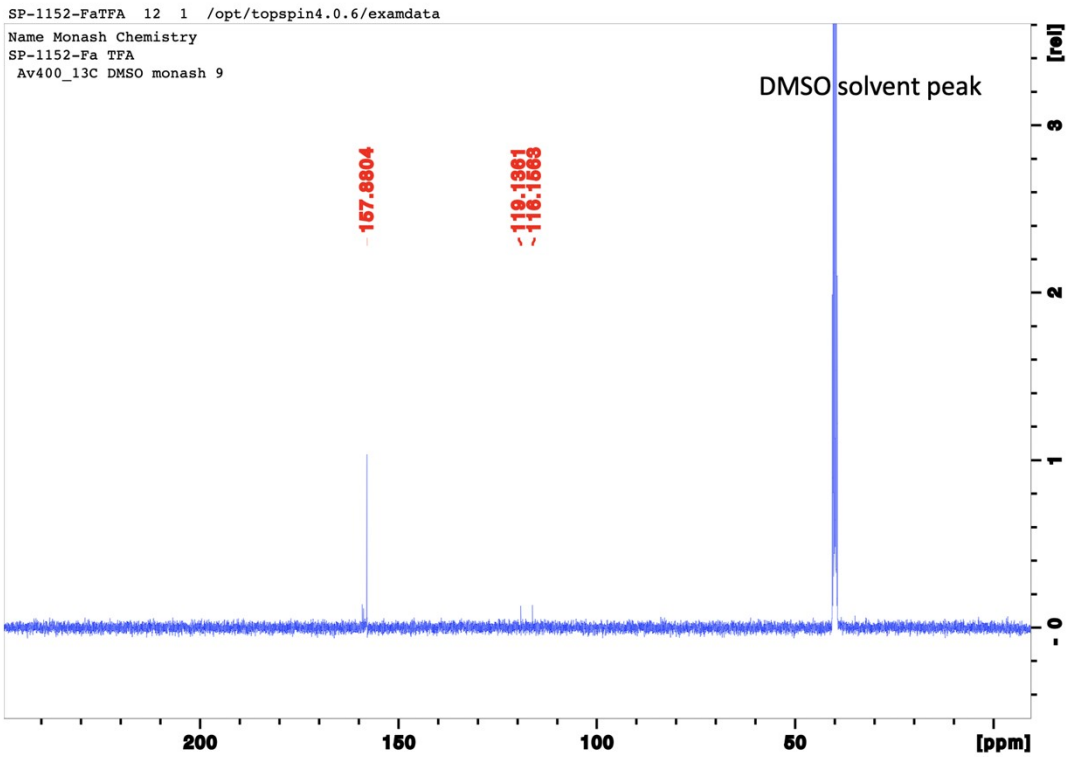

Figure S41. ^{13}C NMR spectrum of [fa][CF_3COO]

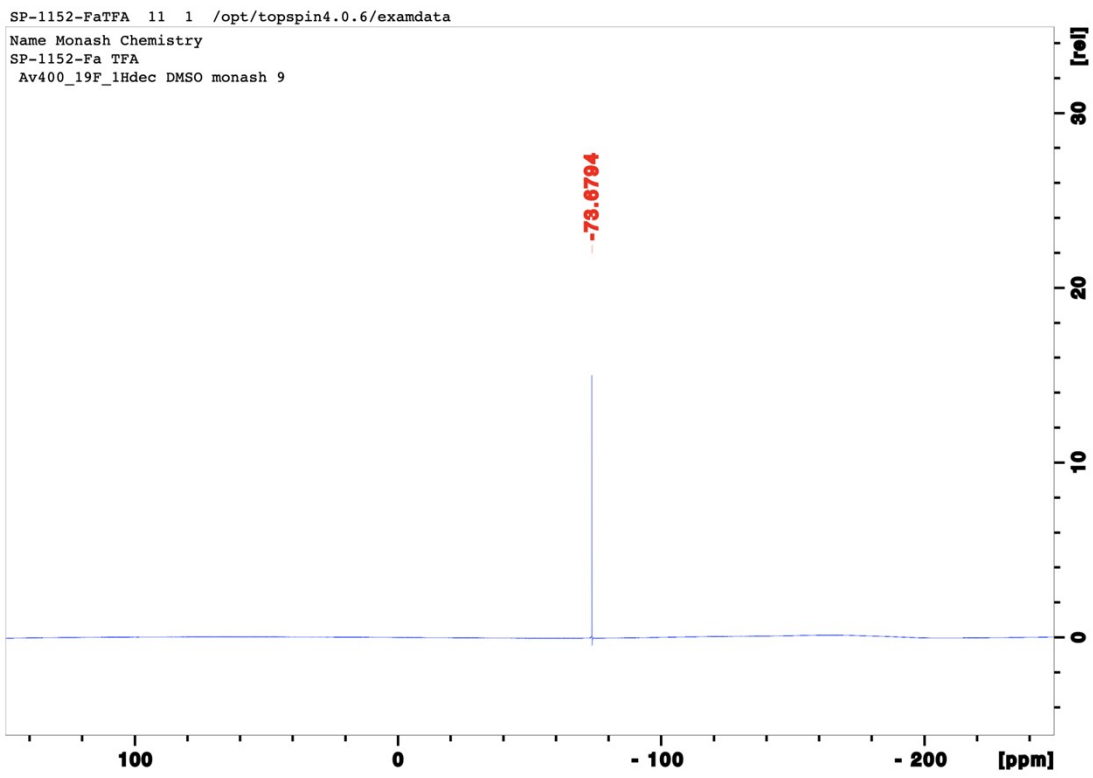

Figure S42. ^{19}F NMR spectrum of [fa][CF_3COO]

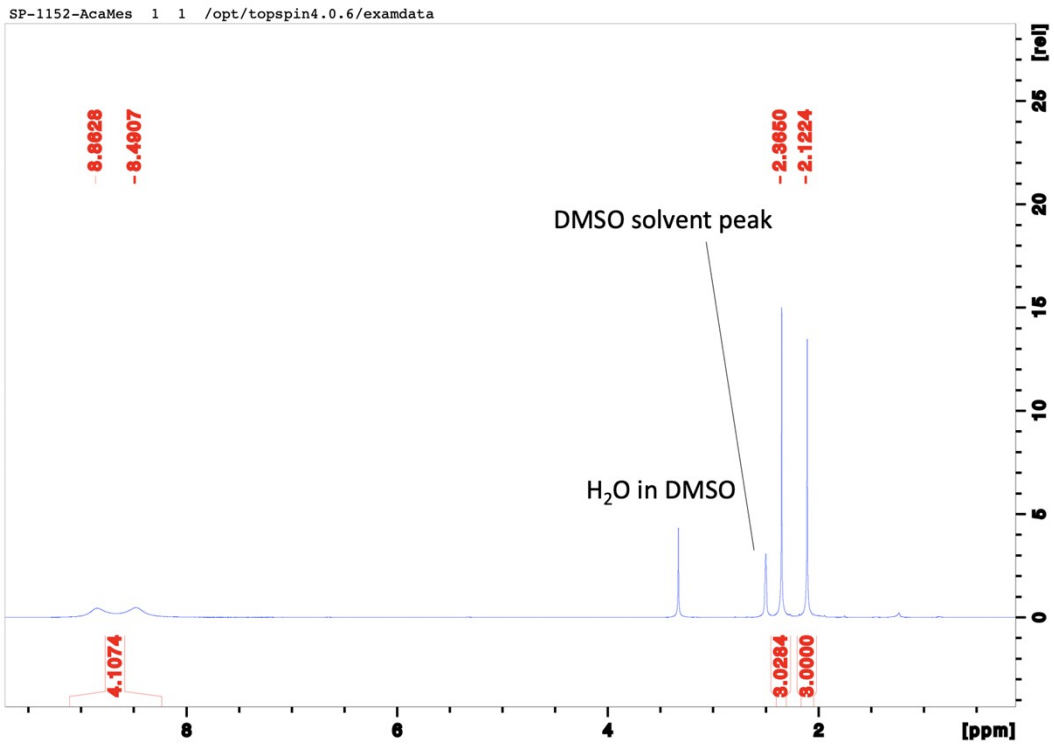

Figure S43. ^{1}H NMR spectrum of [aca][CH_3SO_3]

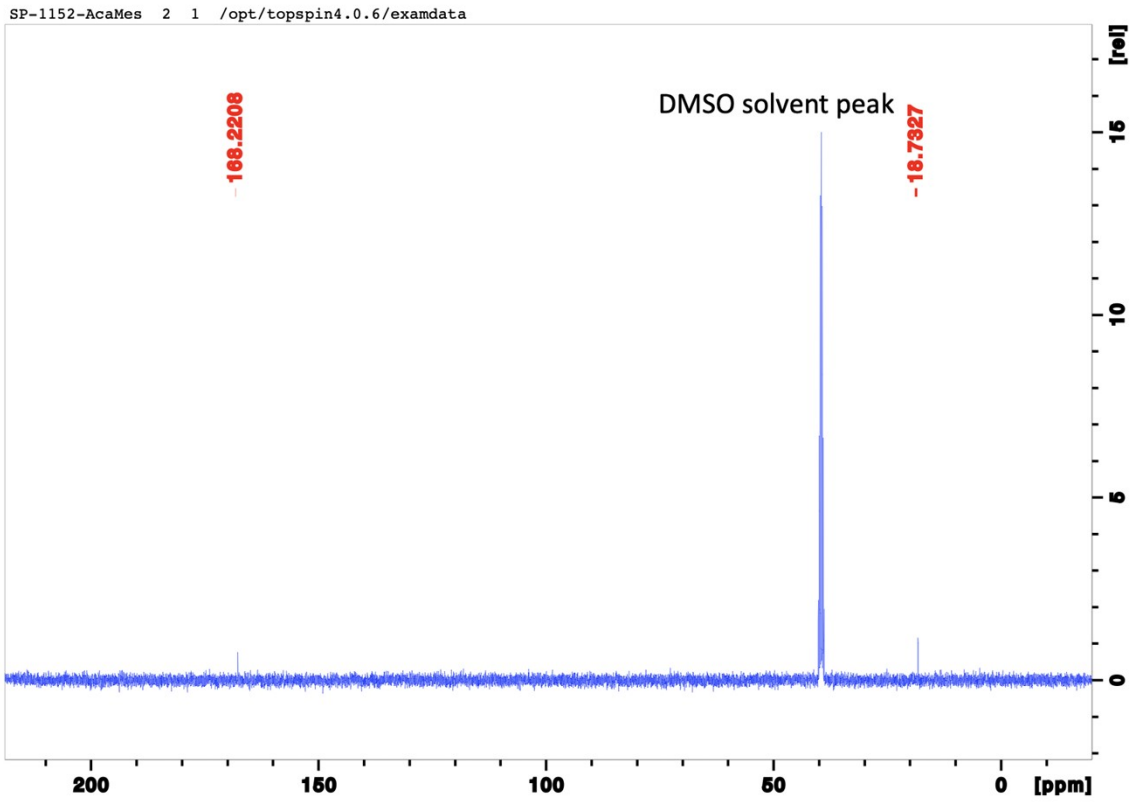

Figure S44. ^{13}C NMR spectrum of [aca][CH_3SO_3]

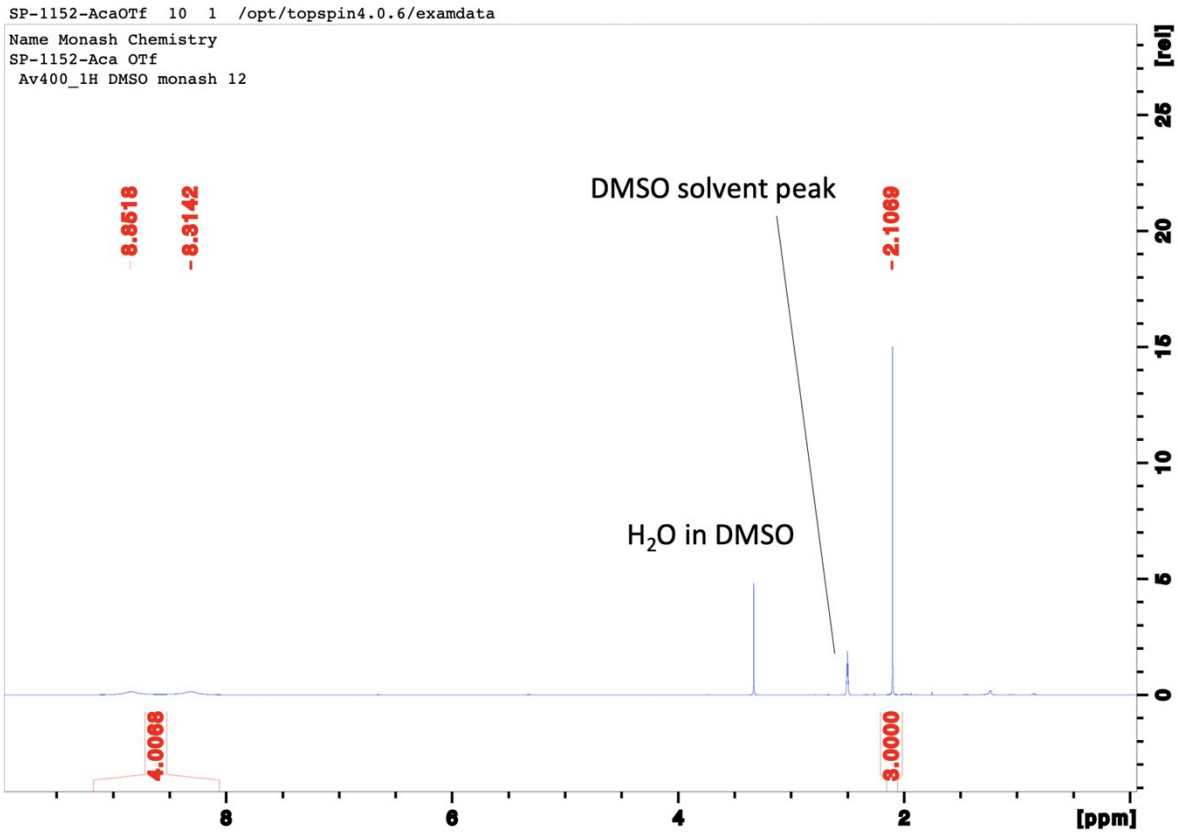

Figure S45. ^{1}H NMR spectrum of [aca][CF_3SO_3]

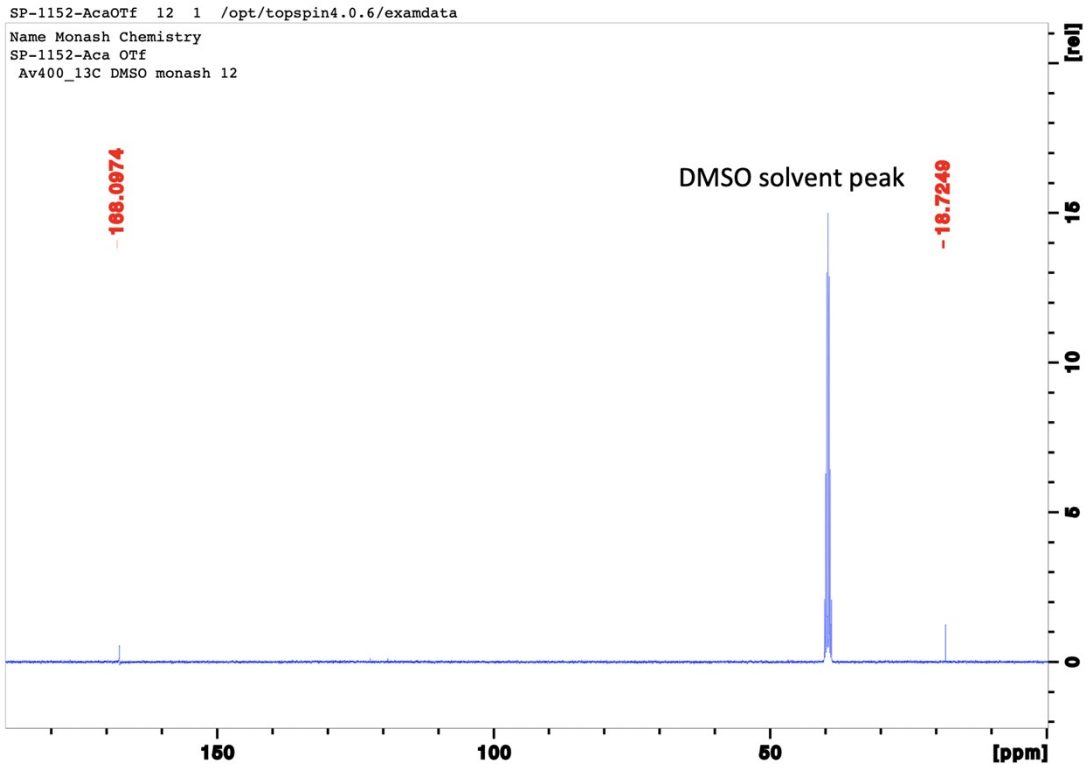

Figure S46. ^{13}C NMR spectrum of [aca][CF_3SO_3]

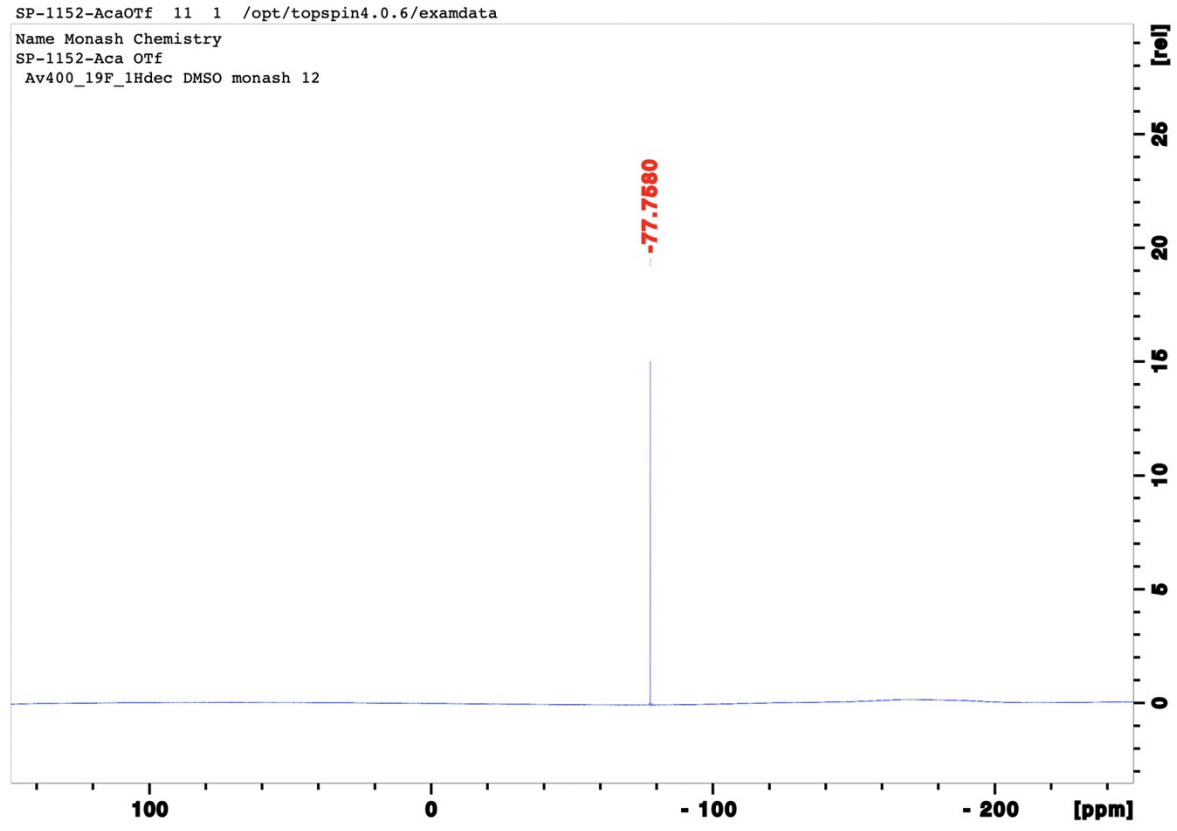

Figure S47. ^{19}F NMR spectrum of [aca][CF_3SO_3]

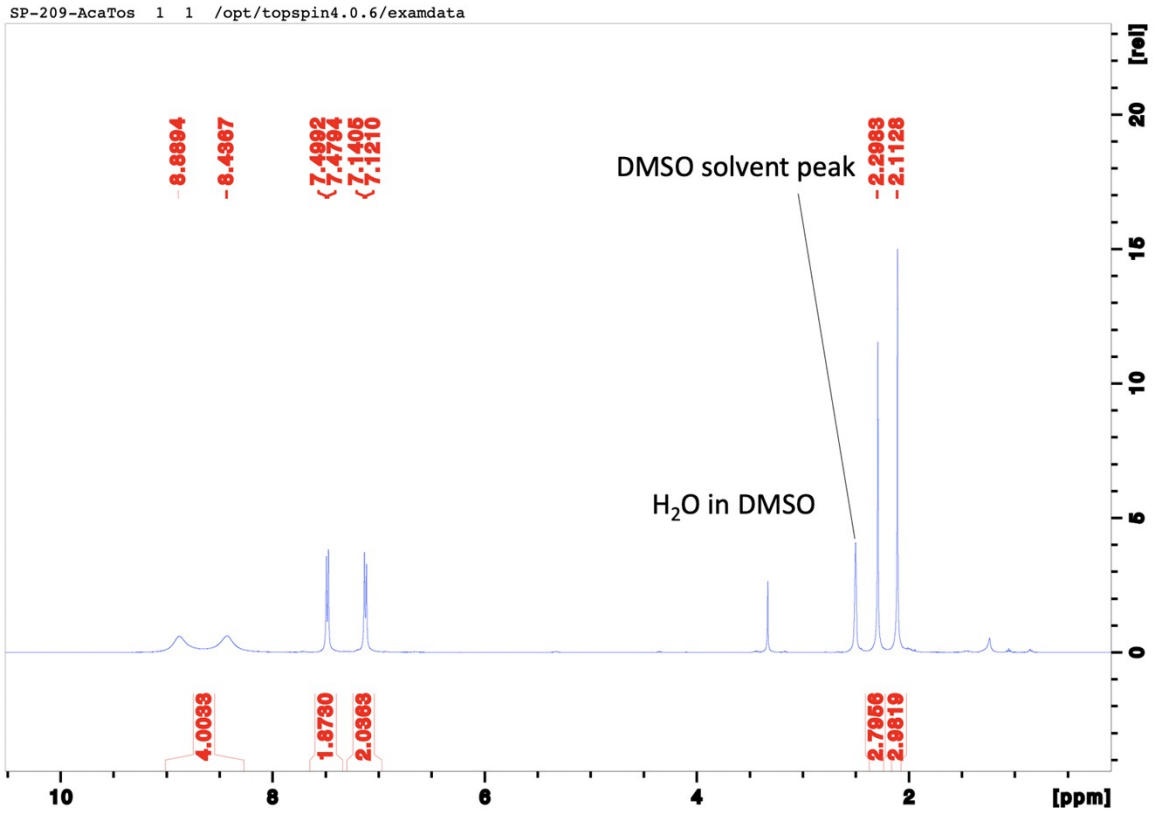

Figure S48. ^{1}H NMR spectrum of [aca][*p*-Tos]

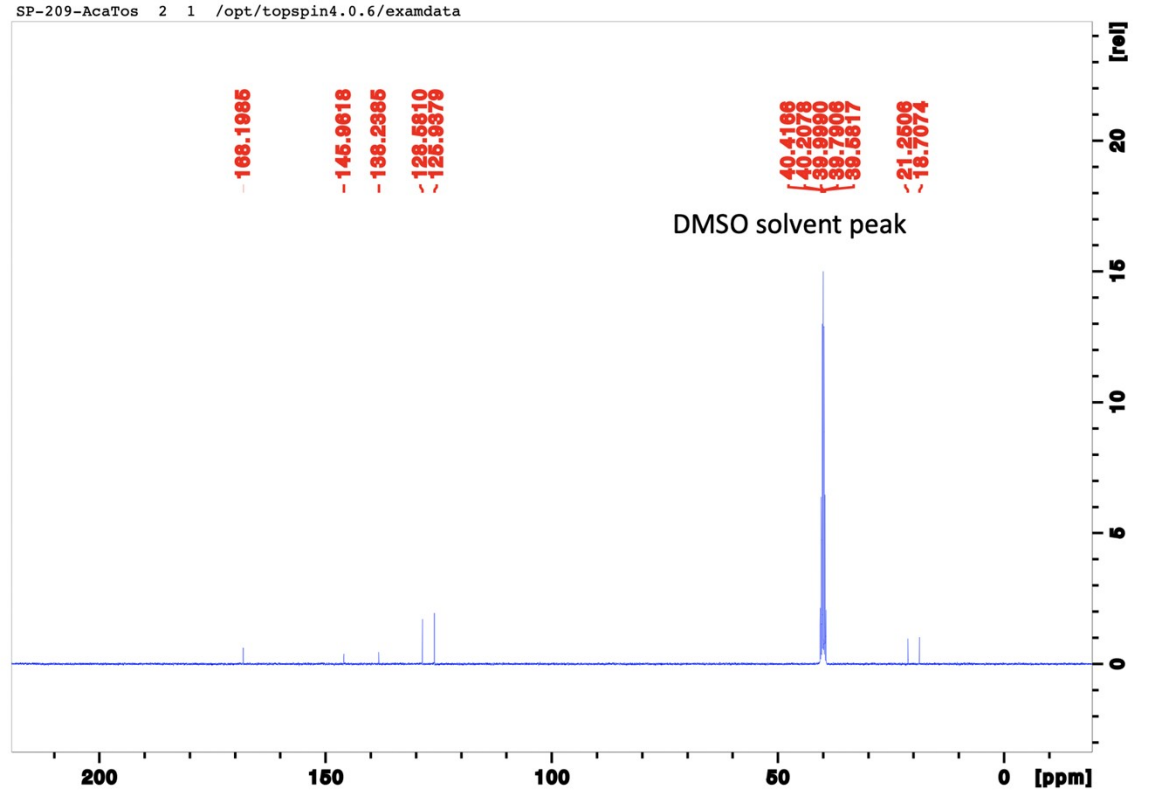

Figure S49. ^{13}C NMR spectrum of [aca][*p*-Tos]

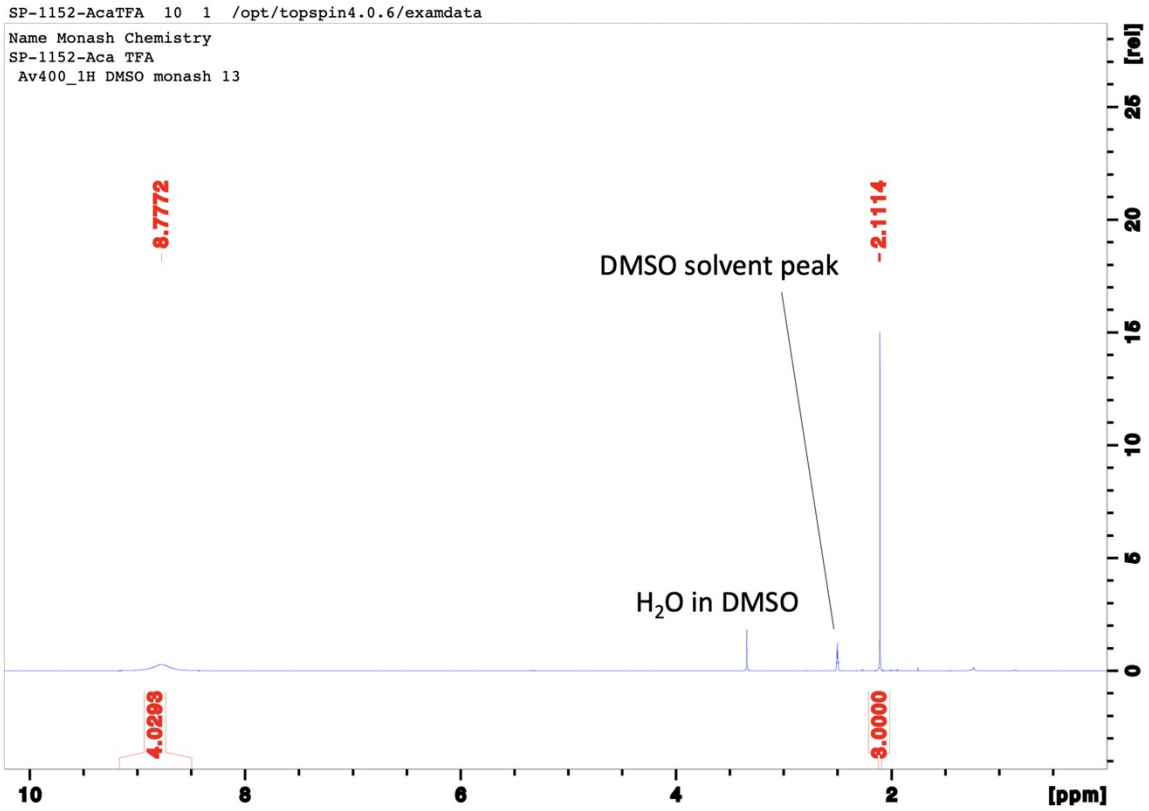

Figure S50. ^{1}H NMR spectrum of [aca][CF_3COO]

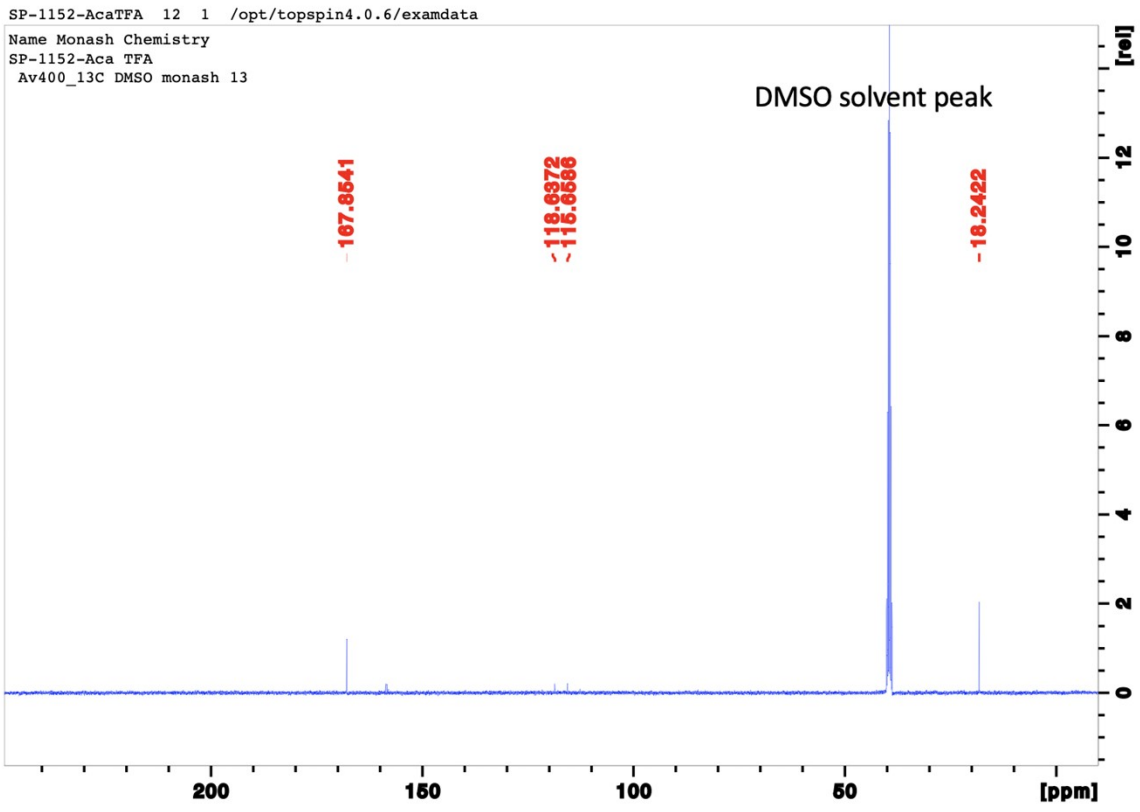

Figure S51. ^{13}C NMR spectrum of [aca][CF_3COO]

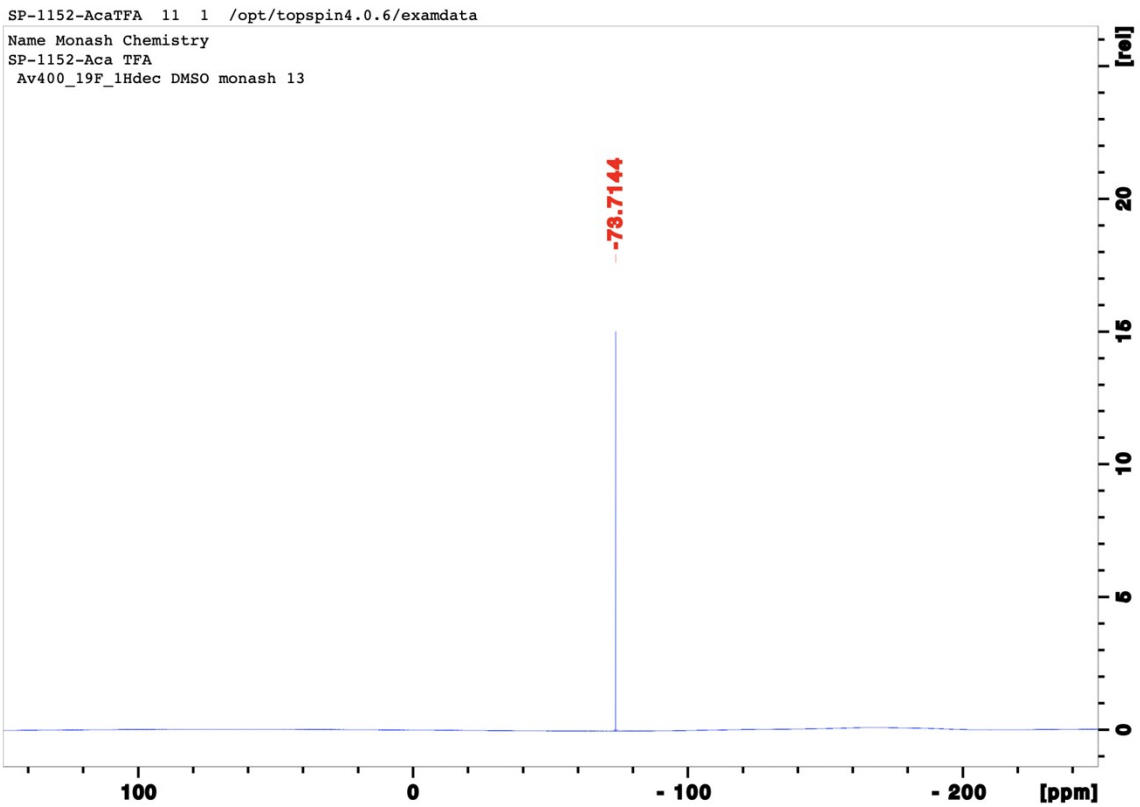

Figure S52. ^{19}F NMR spectrum of [aca][CF_3COO]

References

1 R. Vijayraghavan, U. A. Rana, G. D. Elliott and D. R. MacFarlane, *Energy Technol.*, 2013, **1**, 609–612.

2 J. W. Bats and H. R. Nasiri, CCDC 244747, 2005, DOI:10.5517/cc86p26.

3 V. A. Russell, M. C. Etter and M. D. Ward, *J. Am. Chem. Soc.*, 1994, **116**, 1941–1952.

4 M. Xia, M. Mutailipu, F. Li, Z. Yang and S. Pan, *Cryst. Growth Des.*, 2021, **21**, 1869–1877.

5 D. Dumitrescu, Y.-M. Legrand, F. Dumitrascu, M. Barboiu and A. van der Lee, *Cryst. Growth Des.*, 2012, **12**, 4258–4263.

6 K. Matuszek, R. Vijayaraghavan, M. Kar and D. R. MacFarlane, *Cryst. Growth Des.*, 2019, **20**, 1285–1291.

7 R. Harris and E. Becker, *Pure Appl Chem*, **80**, 59–84.

8 Agilent Technologies Ltd, *CrysAlis PRO*, Agilent, Yarnton, Oxfordshire, England.

9 G. M. Sheldrick, *Acta Crystallogr. Sect. C Struct. Chem.*, 2015, **71**, 3–8.

10 G. M. Sheldrick, *Acta Crystallogr. Sect. Found. Adv.*, 2015, **71**, 3–8.

11 O. V. Dolomanov, L. J. Bourhis, R. J. Gildea, J. A. Howard and H. Puschmann, *J. Appl. Crystallogr.*, 2009, **42**, 339–341.

12 C. F. Macrae, P. R. Edgington, P. McCabe, E. Pidcock, G. P. Shields, R. Taylor, M. Towler and J. Streek, *J. Appl. Crystallogr.*, 2006, **39**, 453–457.

13 C. Shi, B. Wei and W. Zhang, *Cryst. Growth Des.*, 2014, **14**, 6570–6580.